ANALYTICAL AND EXPERIMENTAL STUDIES ON GYROSCOPIC VIBRATION ABSORBERS (PART 1)

AND

ANALYSIS OF PARALLEL DAMPED DYNAMIC VIBRATION ABSORBERS (PART 2)

By A. V. Srinivasan

Prepared under Contract No. NASw-1394 by
KAMAN AIRCRAFT
DIVISION OF KAMAN CORPORATION
Bloomfield, Connecticut

for

NATIONAL AERONAUTICS AND SPACE ADMINISTRATION

ANALYTICAL AND EXPERIMENTAL STUDIES ON GYROSCOPIC VIBRATION ABSORBERS

SUMMARY

A general theoretical analysis is made on three different gyroscopic configurations for possible use as vibration absorbers. The analysis provides for two degrees of translational freedom and three degrees of rotational freedom for the absorber. Computer programs have been written which permit calculations of (1) null and natural frequencies for a given set of parameters; (2) responses in the direction of excitation and orthogonal to it; and (3) responses of the gyro, i.e. angular oscillations of the gyro resulting from vibrations of the structure to which it is connected.

Experimental results have been obtained for two configurations described as "Perissogyro" vibration absorbers. Comparison with corresponding theoretical results indicate reasonable agreement. The analysis and experiments confirm the possibility of obtaining antiresonance in two orthogonal directions simultaneously. Details of electronic circuitry required to synchronize the gyro speed with the excitation frequency are presented.

This study, while confirming the feasibility of gyroscopic systems for use as Synchronous Vibration Absorbers, has brought to light certain practical problems that are likely to be encountered during actual use. These problems observed during experimentation pertain (1) to the conditions of self-excited oscillations of "Perissogyro" vibration absorbers; and (2) to the apparent transfer of energy to a yaw motion of the device when vibration in orthogonal directions are simultaneously nulled. A general discussion of these problems together with recommendations for further research is presented.

This report is in two parts. The first part discusses Synchronous Vibration Absorbers. The second part is devoted to an analytical study of parallel absorbers, where the absorber consists of an undamped mass together with a damped mass. The summary of research pertaining to the second part is presented separately in Part 2.

TABLE OF CONTENTS

	Page
SUMMARY.	ii
TABLE OF CONTENTS.	iii
INTRODUCTION	1
PART 1	7
LIST OF SYMBOLS	8
LIST OF FIGURES	10
ANALYSIS.	11
ALTERNATE CONFIGURATION OF THE "PERISSOGYRO VIBRATION ABSORBER"	29
CORIOLIS VIBRATION ABSORBER	35
EXPERIMENTAL SETUP AND PROCEDURES	39
RESULTS AND DISCUSSION.	50
GYROSPEED SYNCHRONIZATION FOR "PERISSOGYRO VIBRATION ABSORBER"	57
PART 2	61
LIST OF SYMBOLS	62
LIST OF FIGURES	64
SUMMARY	65
INTRODUCTION.	66
ANALYSIS.	67
DISCUSSION AND CONCLUSIONS.	77
ACKNOWLEDGEMENTS.	86

INTRODUCTION

The concept of vibration absorbers can be traced back to 1909 when H. Frahm invented a simple device which is commonly referred to as the conventional dynamic vibration absorber. In its simplest form, the Frahm absorber consists of an auxiliary undamped spring-mass system attached to the vibrating mass at a point where it is required to react the effective excitation force. If the natural frequency of the absorber mass is chosen to be equal to the frequency of the excitation force, then the main mass does not vibrate at all and is said to attain a null. Although Frahm absorbers are quite popular in use because of their simplicity, their effectiveness is rather limited to situations where the excitation frequency is nearly constant. In fact, the addition of an absorber mass introduces another degree of freedom to the system and thus another resonant condition which might do more harm than good. In general, the excitation frequency varies over a range which renders the conventional absorbers useless.

The purpose of many investigations that have followed since the introduction of Frahm absorbers has been either:

(1) to invent entirely new and better devices in the hope of replacing the conventional absorber, or

(2) to improve the effectiveness of the conventional absorber by suitable modification.

Pendulum absorbers, impact dampers, gyroscopic vibration absorbers are but a few of the new devices that belong to the former group. However, the only modification considered so far in the latter group is the addition of damping to the absorber mass.

Part 1 of this report presents the theoretical analysis of three configurations of gyroscopic vibration absorbers. Also, experimental results are included for two configurations. The purpose of Part 2 of this report is to examine a modification of the conventional absorber. Such a modification consists of adding, in parallel, a subsidiary undamped absorber mass in addition to the damped absorber mass.

The idea of utilizing gyroscopic effects which result in a completely inertial/conservative means of reacting a sinusoidal force originated in the Kaman Vibrations Research Group. The invention which is patented as Gyroscopic Vibration Absorbers is due to W. G. Flannelly[1] of the Vibrations Research Group at Kaman Aircraft, Division of Kaman Corporation. Preliminary research on gyroscopic vibration absorbers conducted under a contract for the National Aeronautics and Space Administration has already been reported[2].

The analysis presented in Reference 2 established the unique characteristics of gyroscopic systems used as vibration absorbers. For example, it is shown that gyroscopic vibration absorbers lend themselves to synchronization so that the gyro speed may be made to adjust itself suitably when the forcing frequency varies. This obviously is a tremendous advantage in that these devices can theoretically provide an infinite bandwidth so that a null is always attained no matter what the driving frequency is. Admittedly more tests and a thorough parametric study are necessary before the device is developed and put to actual use. However, the potentials of gyroscopic configurations for use as dynamic absorbers appear to be very promising. Further, the possibility of using two absorbers in parallel, one damped and the other undamped, has shown that it is possible to obtain an undamped null in a dynamic absorber system which exhibits a well-damped peak. These and other aspects of gyroscopic vibration absorbers and parallel damped absorbers are examined in considerable detail in the present investigation.

Figures 1, 2 and 3 show three of the possible configurations of gyroscopic systems to which the theory presented in Part 1 of this report is applicable. In Figure 1, the gyro wheel, the drive system, the cross pivots, all rotate in unison. Such a device is designated as "Perissogyro Vibration Absorber".

In Figure 2 is shown a device which is similar to the configuration shown in Figure 1 in all but one respect, i.e. the gyro-wheel in this case can rotate relative to the drive system. Figure 3 shows a configuration in which two inertial elements are arranged such that their pivotal axes are at right angles to each other. As in Figure 1, the inertial elements and the pivotal axes rotate together. This device is designated here as "Coriolis Vibration Absorber".

[1] "Gyroscopic Vibration Absorber" by William G. Flannelly, U.S. Patent No. 3,313,163, 11 April 1967.

[2] "Analytical Research on a Synchronous Vibration Absorber" by William G. Flannelly and John C. Wilson, NASA Contractor Report CR-338, December 1965.

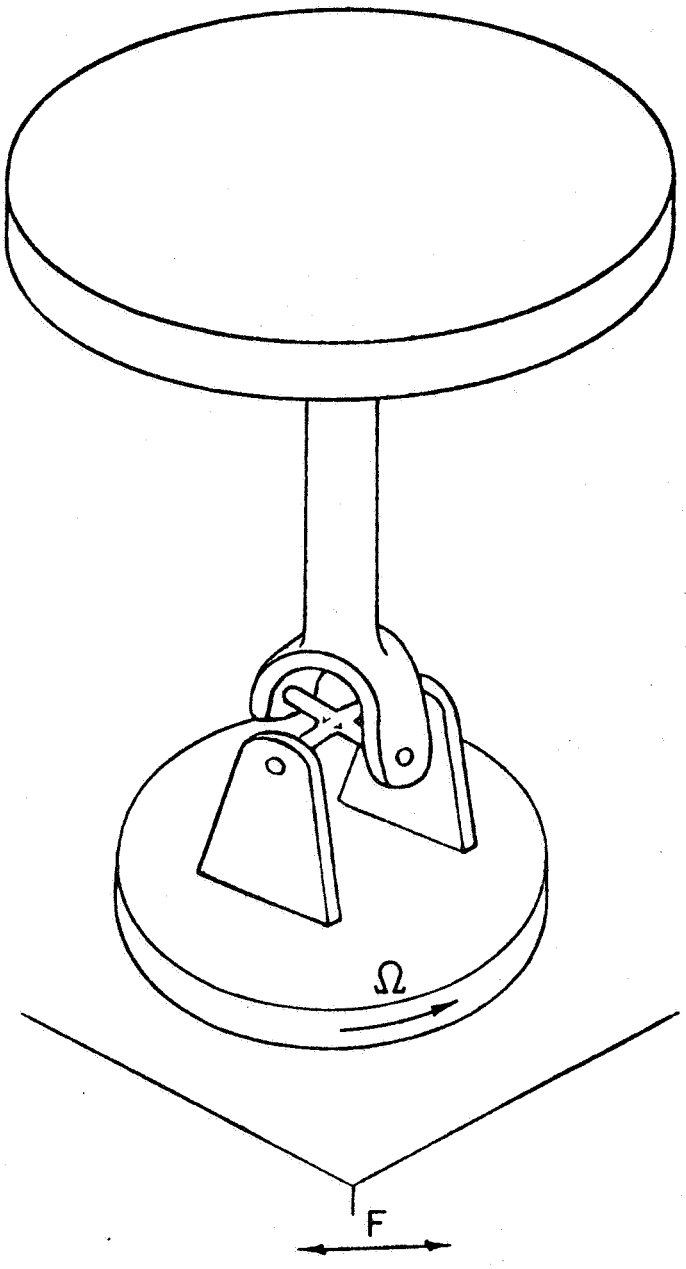

Figure 1. The Perissogyro Vibration Absorber

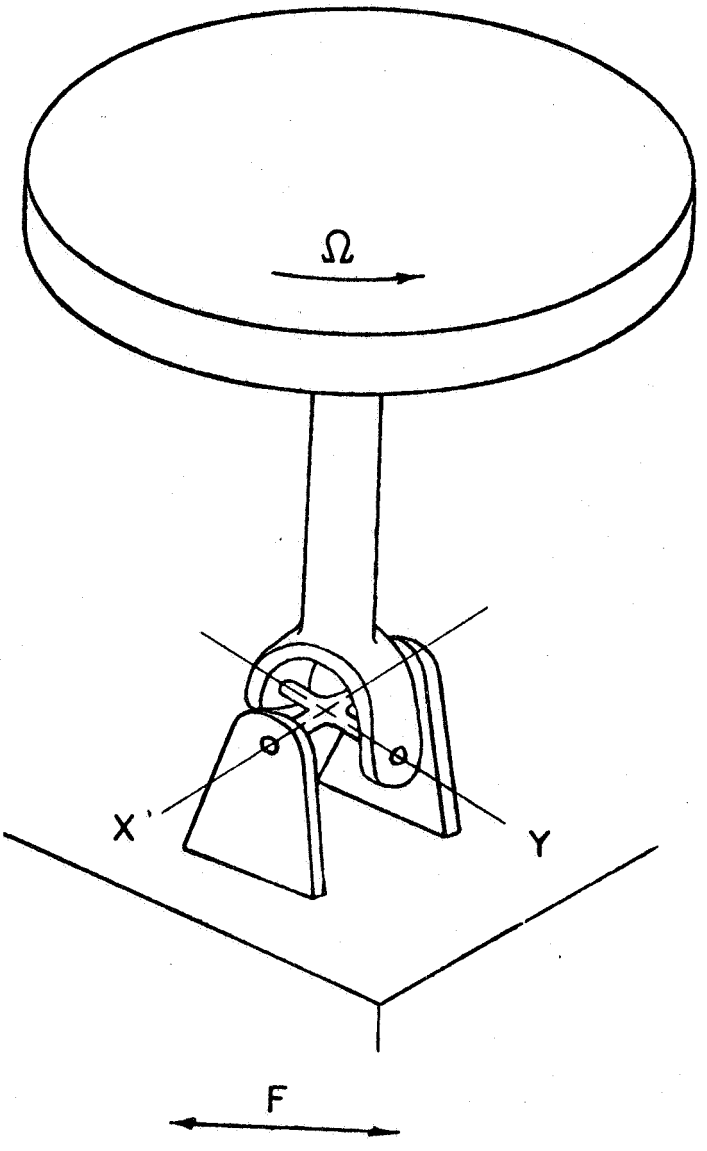

Figure 2. Alternate Configuration of the Perissogyro Vibration Absorber

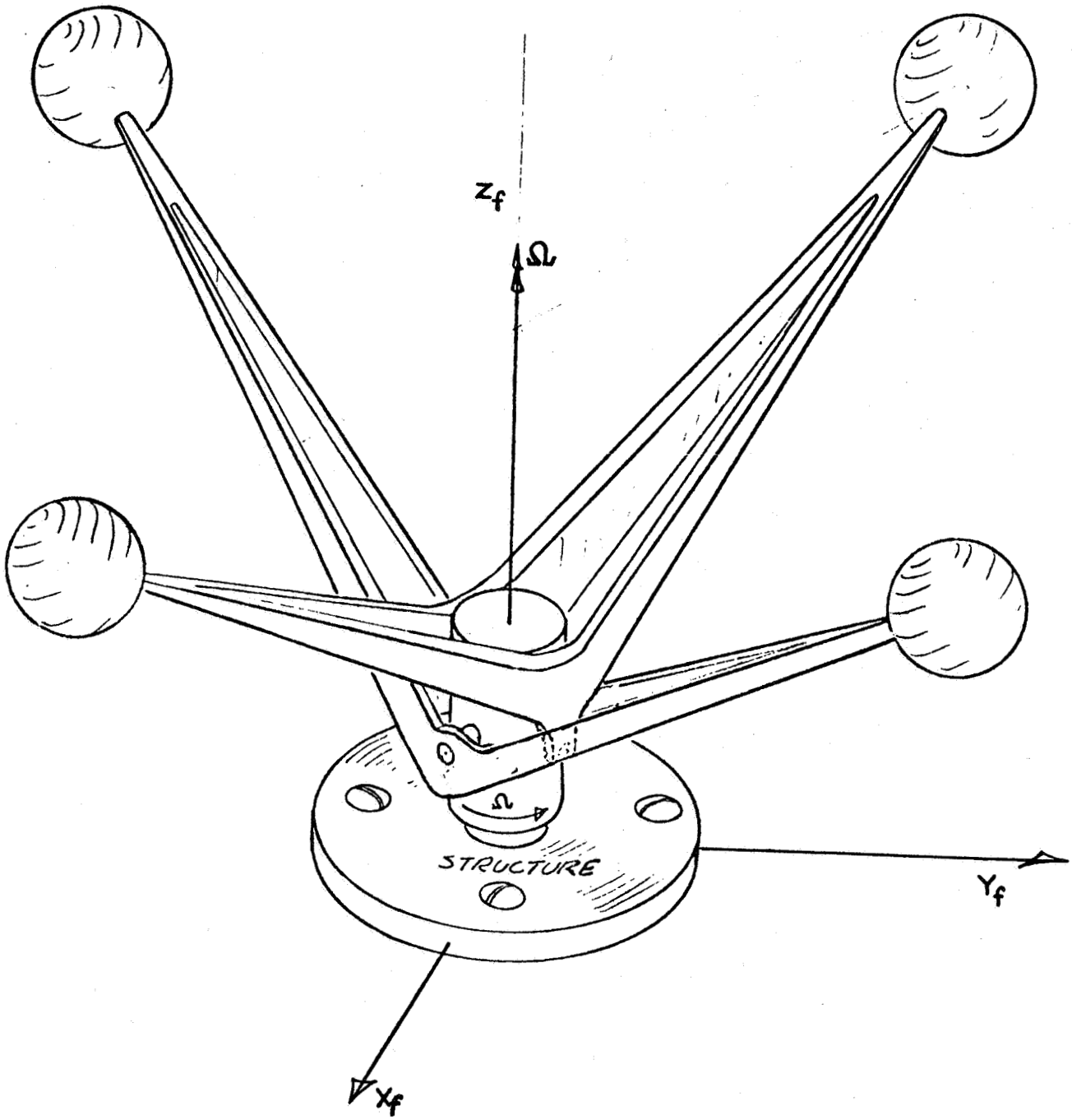

Figure 3. Coriolis Vibration Absorber

In this report, the governing equations of motion for all the configurations are derived using Lagrangian technique. The approach used in this investigation is different from the conventional procedures in that the body attitudes are referred to a fixed frame of reference as opposed to Euler's description of motion in terms of body angular rates. The analysis is quite general and assumes two degrees of translational freedom and three degrees of rotational freedom for the gyroscopic systems. Spring rates are included in the analysis for all pivots and along the translational degrees of freedom. The resulting equations of motion are a coupled set of nonlinear ordinary differential equations for each gyroscopic configuration.

Several simplifying assumptions, based on the fact that the devices treated here should be of practical use, reduce the governing equations to a set of linear differential equations, the solutions for which can be written readily. Numerical results, obtained during the study, are presented graphically. The relative merits of the devices considered here are discussed briefly.

The circuitry needed to obtain linear synchronization in Perissogyro Absorbers has been designed, and a brief discussion provided in the report.

PART 1

LIST OF SYMBOLS

f_X	Forcing function along the X axis
h	Distance of the centroid of the gyro disc from the pivots
I	Moment of inertia of the gyroscopic system
K_X	Spring rate along X direction
K_Y	Spring rate along Y direction
K	Spring rate in the pivots
L	Lagrangian
M	Mass of the gyro disc
$\overline{M}$	Total mass of the absorber including the effective mass of the structure
0	Origin of the fixed frame of reference
t	Time coordinate
X_f Y_f Z_f	Coordinate axes in the fixed frame of reference
X_b Y_b Z_b	Coordinate axes fixed to the gyro disc

LIST OF SYMBOLS (Continued)

ψ θ φ	Euler angle coordinates
Ω	Spin velocity of the gyro disc
Ψ Θ Φ	Matrices of transformation
η ζ	Transformed coordinates

LIST OF FIGURES

Figure		Page
1	The Perissogyro Vibration Absorber	1
2	Alternate Configuration of the Perissogyro Vibration Absorber	4
3	Coriolis Vibration Absorber	5
4	Coordinate Transformation	12
5	Coordinate Transformation	29
6	Schematic of the Experimental Setup	40
7	Photograph of the Experimental Setup of the Perissogyro Vibration Absorber	41
8	Determination of the Lateral Spring Rate	42
9	Null-RPM Characteristics of Perissogyro Vibration Absorbers	44
10	Photograph of the Experimental Setup of the Double Perissogyro Vibration Absorber	45
11	Example of Traces Obtained by Experiment on Double Perissogyro Absorber	46
12	Example of Traces Obtained by Experiment on Double Perissogyro Absorber	47
13	Theoretical and Experimental Response Curves (1800 rpm)	51
14	Theoretical and Experimental Response Curves (3600 rpm)	52
15	Example of a Trace Obtained by Experiment on Perissogyro Vibration Absorber	53
16	Theoretical and Experimental Response Curves for the Double Perissogyro Vibration Absorber	55
17	Theoretical and Experimental Response Curves for the Double Perissogyro Vibration Absorber	56
18	Circuitry for Linear Synchronization of Gyro Speed	60

ANALYSIS

"Perissogyro Vibration Absorber"

Figure 4 represents a fixed coordinate system of reference X_f, Y_f, Z_f which cannot rotate but can translate in the X_f, Y_f directions.

The coordinate system X_b, Y_b, Z_b whose origin coincides with that of the fixed system is fixed to the body of the gyro and moves with it. The center of gravity of the rigid body is assumed to be located at "h" units from the origin . The final position of an element of mass dm at any instant may be expressed in terms of the fixed system coordinates. The body assumes its final position at instant "t" through a set of three Euler-angle rotations given in the following sequence: rotation ψ about Z_f, rotation Θ about Y_1 (i.e. rotated Y axis) and finally rotation ϕ about X_b (i.e. rotated X axis). In addition, the rigid body may undergo translations in the X_f and Y_f directions.

Representing the matrices of transformation associated with the Euler-angle rotations ψ , θ and ϕ by Ψ , Θ and Φ , the coordinates of a mass particle referred to the fixed system may be expressed in terms of the body coordinates by the matrix equation.

$$\begin{Bmatrix} X_f \\ Y_f \\ Z_f \end{Bmatrix} = \left(\Psi \Theta \Phi \right) \begin{Bmatrix} X_b \\ Y_b \\ Z_b \end{Bmatrix} \tag{1}$$

Where

$$\Psi = \begin{pmatrix} \cos\psi & -\sin\psi & 0 \\ \sin\psi & \cos\psi & 0 \\ 0 & 0 & 1 \end{pmatrix} \tag{2}$$

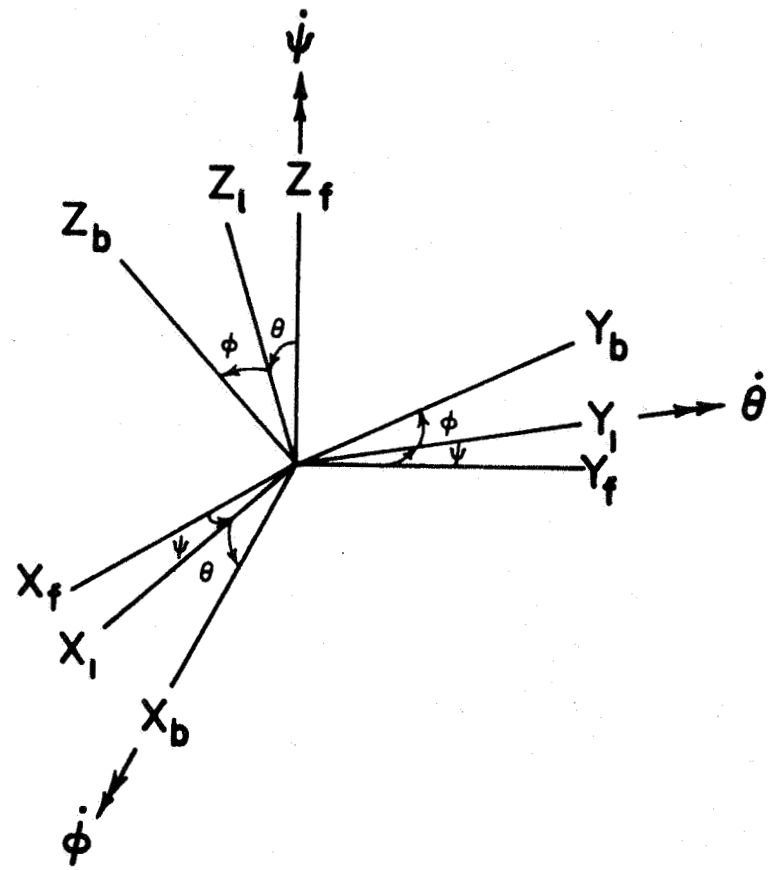

Figure 4. Coordinate Transformation

$$\Theta = \begin{pmatrix} \cos\theta & 0 & \sin\theta \\ 0 & 1 & 0 \\ -\sin\theta & 0 & \cos\theta \end{pmatrix} \tag{3}$$

and

$$\Phi = \begin{pmatrix} 1 & 0 & 0 \\ 0 & \cos\varphi & -\sin\varphi \\ 0 & \sin\varphi & \cos\varphi \end{pmatrix} \tag{4}$$

Upon multiplication of the matrices $\Psi \Theta \Phi$, X_f, Y_f and Z_f may be shown to be

$$\begin{aligned} X_f &= X_o + X_b C_\theta C_\psi + Y_b (S_\varphi S_\theta C_\psi - S_\psi C_\varphi) + Z_b (S_\varphi S_\psi + S_\theta C_\psi C_\varphi) \\ Y_f &= Y_o + X_b C_\theta S_\psi + Y_b (S_\varphi S_\theta S_\psi + C_\psi C_\varphi) + Z_b (S_\theta S_\psi C_\varphi - S_\varphi C_\psi) \\ Z_f &= -X_b S_\theta + Y_b S_\varphi C_\theta + Z_b C_\theta C_\varphi \quad , \end{aligned} \tag{5}$$

where S_ψ represents $\sin\psi$, C_ψ represents $\cos\psi$ and so on for the other variables θ and φ. It may be noted that the displacements X_o and Y_o in the X_f and Y_f directions have been added to the appropriate equations of transformation. With the coordinates of any mass particle in the rigid body expressed in terms of the fixed system coordinates, the velocities $\dot{X}_f$, $\dot{Y}_f$ and $\dot{Z}_f$ may be computed. Thus

$$\begin{aligned} \dot{X}_f &= \dot{X}_o + \alpha_1 X_b + \beta_1 Y_b + \gamma_1 Z_b \\ \dot{Y}_f &= \dot{Y}_o + \alpha_2 X_b + \beta_2 Y_b + \gamma_2 Z_b \\ \dot{Z}_f &= \alpha_3 X_b + \beta_3 Y_b + \gamma_3 Z_b \end{aligned} \tag{6}$$

where

$$\alpha_1 = -(S_\psi C_\theta \dot{\psi} + C_\psi S_\theta \dot{\theta})$$

$$\alpha_2 = C_\psi C_\theta \dot{\psi} - S_\psi S_\theta \dot{\theta}$$

$$\alpha_3 = -C_\theta \dot{\theta}$$

$$-\beta_1 = (C_\psi C_\varphi + S_\psi S_\theta S_\varphi)\dot{\psi} - C_\psi C_\theta S_\varphi \dot{\theta} - (C_\psi S_\theta C_\varphi + S_\psi S_\varphi)\dot{\varphi}$$

$$\beta_2 = (C_\psi S_\theta S_\varphi - S_\psi C_\varphi)\dot{\psi} + S_\psi C_\theta S_\varphi \dot{\theta} + (S_\psi S_\theta C_\varphi - C_\psi S_\varphi)\dot{\varphi}$$

$$\beta_3 = C_\theta C_\varphi \dot{\varphi} - S_\theta S_\varphi \dot{\theta}$$

$$\gamma_1 = (C_\psi S_\varphi - S_\psi S_\theta C_\varphi)\dot{\psi} + C_\psi C_\theta C_\varphi \dot{\theta} + (S_\psi C_\varphi - C_\psi S_\theta S_\varphi)\dot{\varphi}$$

$$\gamma_2 = (S_\psi S_\varphi + C_\psi S_\theta C_\varphi)\dot{\psi} + S_\psi C_\theta C_\varphi \dot{\theta} - (S_\psi S_\theta S_\varphi + C_\psi C_\varphi)\dot{\varphi}$$

$$-\gamma_3 = S_\theta C_\varphi \dot{\theta} + C_\theta S_\varphi \dot{\varphi} \qquad (7)$$

The expression for the total kinetic energy may now be derived by calculating

$$T = \frac{1}{2} \int (\dot{X}_f^2 + \dot{Y}_f^2 + \dot{Z}_f^2)\, dm \qquad (8)$$

The calculations to obtain T are rather laborious but straightforward. Omitting the details of algebraic manipulations, $\dot{X}_f^2 + \dot{Y}_f^2 + \dot{Z}_f^2$ may be shown to be (omitting the subscripts on x_b, Y_b, z_b)

$$\dot{X}_o^2 + \dot{Y}_o^2 + \dot{\psi}^2 \left\{ C_\theta^2 x^2 + (C_\varphi^2 + S_\varphi^2 S_\theta^2) Y^2 + (S_\varphi^2 + C_\varphi^2 S_\theta^2) Z^2 \right\} +$$

$$\dot{\theta}^2 \left\{ x^2 + S_\varphi^2 y^2 + C_\varphi^2 z^2 \right\} + \dot{\varphi}^2 \left\{ y^2 + z^2 \right\} - 2 C_\theta S_\varphi C_\varphi \dot{\psi} \dot{\theta} (Y^2 - Z^2)$$

$$- 2 S_\theta \dot{\psi} \dot{\varphi} (Y^2 + Z^2) + 2Z \Big[\dot{X}_o \left\{ (C_\psi S_\varphi - S_\psi S_\theta C_\varphi) \dot{\psi} + \right.$$

$$C_\psi C_\theta C_\varphi \dot{\theta} + (S_\psi C_\varphi - C_\psi S_\theta S_\varphi) \dot{\varphi} \Big\} + \dot{Y}_o \left\{ (S_\psi S_\varphi + C_\psi S_\theta C_\varphi) \dot{\psi} \right.$$

$$\left. + S_\psi C_\theta C_\varphi \dot{\theta} - (S_\psi S_\theta S_\varphi + C_\psi C_\varphi) \dot{\varphi} \right\} \Big] \quad . \tag{9}$$

The potential energy stored in the system is assumed to be solely due to the spring rates in the pivots and along the X_f and Y_f directions, i.e. the contribution to the total potential energy from gravitational forces is neglected in the analysis. Thus, the expression for V may be written as

$$V = \frac{1}{2} \left\{ K_\theta \theta^2 + K_\varphi \varphi^2 + K_X X_o^2 + K_Y Y_o^2 \right\} \tag{10}$$

where K_θ, K_φ are the spring rates in the pivots along the θ and φ directions, and K_X, K_Y represent the spring rates along the X, Y directions.

The body axes are assumed to be along the principal axes of inertia of the rigid body. Thus, in calculating the kinetic energy integral from Equation (8), all the product of inertia terms are assumed to be identically zero.

The governing equations of motion in terms of the generalized coordinates $\psi, \theta, \varphi, X_o$ and Y_o may now be derived from the Lagrangian L, using

$$\frac{d}{dt} \frac{\partial L}{\partial \dot{q}_i} - \frac{\partial L}{\partial q_i} = Q_i \tag{11}$$

where q_i is a generalized coordinate and Q_i the corresponding generalized force. The resulting equations are a set of coupled nonlinear ordinary differential equations and are given below.

$$\begin{cases} \ddot{\psi}\left(C_\theta^2 S_\varphi^2 I_y + S_\theta^2 I_x + C_\theta^2 C_\varphi^2 I_z\right) + \ddot{\theta}\, C_\theta C_\varphi S_\varphi \left(I_y - I_z\right) - \ddot{\varphi}\, S_\theta I_x + \dot{\theta}^2 \left(I_z - I_y\right) S_\theta S_\varphi C_\varphi + \\ 2\dot{\psi}\dot{\theta}\left\{C_\theta S_\theta \left(I_x - I_z C_\varphi^2 - I_y S_\varphi^2\right)\right\} + 2\dot{\psi}\dot{\varphi}\left(I_y - I_z\right) S_\varphi C_\varphi C_\theta^2 - 2\dot{\varphi}\dot{\theta}\, C_\theta \left\{S_\varphi^2 \left(I_z - I_y\right) + \tfrac{1}{2}\left(I_x + I_y - I_z\right)\right\} + \\ Mh\left\{\ddot{X}_o\left(C_\psi S_\varphi - S_\psi S_\theta C_\varphi\right) + \ddot{Y}_o\left(S_\psi S_\varphi + C_\psi C_\varphi S_\theta\right)\right\} = Q_\psi \end{cases}$$

$$\begin{cases} \ddot{\phi} I_x - \ddot{\psi} S_\theta I_x + \dot{\psi}^2 \left(I_z - I_y\right) C_\theta^2 S_\varphi C_\varphi + \dot{\theta}^2 \left(I_y - I_z\right) S_\varphi C_\varphi - \dot{\psi}\dot{\theta}\left\{I_x + \left(I_y - I_z\right)\left(C_\varphi^2 - S_\varphi^2\right)\right\} + \\ Mh\left\{\ddot{X}_o\left(S_\psi C_\varphi - C_\psi S_\theta S_\varphi\right) - \ddot{Y}_o\left(S_\psi S_\theta S_\varphi + C_\psi C_\varphi\right)\right\} + K_\varphi \varphi = Q_\varphi \end{cases} \qquad (12)$$

$$\begin{cases} \ddot{\theta}\left(C_\varphi^2 I_y + S_\varphi^2 I_z\right) + \ddot{\psi}\left(I_y - I_z\right) C_\theta C_\varphi S_\varphi + \dot{\psi}^2 C_\theta S_\theta \left(I_y S_\varphi^2 + I_z C_\varphi^2 - I_x\right) + \dot{\psi}\dot{\varphi} C_\theta \left\{I_x + \left(I_y - I_z\right)\left(C_\varphi^2 - S_\varphi^2\right)\right\} \\ + 2\dot{\varphi}\dot{\theta}\left(I_z - I_y\right) S_\varphi C_\varphi + Mh\left(\ddot{X}_o C_\psi C_\theta C_\varphi + \ddot{Y}_o C_\theta S_\psi C_\varphi\right) + K_\theta \theta = Q_\theta \end{cases}$$

$$\begin{cases} \bar{\bar{M}}\ddot{X}_o + Mh\left\{\ddot{\psi}\left(C_\psi S_\varphi - S_\psi S_\theta C_\varphi\right) + \ddot{\theta} C_\psi C_\theta C_\varphi + \ddot{\varphi}\left(S_\psi C_\varphi - C_\psi S_\theta S_\varphi\right) - \dot{\psi}^2\left(S_\psi S_\varphi + S_\theta C_\psi C_\varphi\right) - \right. \\ \left. \dot{\theta}^2 C_\psi S_\theta C_\varphi - \dot{\varphi}^2\left(S_\psi S_\varphi + C_\psi S_\theta C_\varphi\right) - 2\dot{\psi}\dot{\theta} S_\psi C_\theta C_\varphi - 2\dot{\varphi}\dot{\theta}\, C_\varphi C_\theta S_\varphi + 2\dot{\varphi}\dot{\psi}\left(C_\psi C_\varphi + S_\psi S_\theta S_\varphi\right)\right\} + K_x X_o = f_x \end{cases}$$

$$\begin{cases} \bar{\bar{M}}\ddot{Y}_o + Mh\left\{\ddot{\psi}\left(S_\psi S_\varphi + C_\psi S_\theta C_\varphi\right) + \ddot{\theta} S_\psi C_\theta C_\varphi - \ddot{\varphi}\left(C_\psi C_\varphi + S_\psi S_\theta S_\varphi\right) + \dot{\psi}^2\left(C_\psi S_\varphi - S_\psi S_\theta C_\varphi\right) - \right. \\ \left. \dot{\theta}^2 S_\psi S_\theta C_\varphi - \dot{\varphi}^2\left(S_\psi S_\theta C_\varphi - C_\psi S_\varphi\right) + 2\dot{\psi}\dot{\theta} C_\psi C_\theta C_\varphi - 2\dot{\varphi}\dot{\theta} S_\psi C_\theta S_\varphi + 2\dot{\varphi}\dot{\psi}\left(S_\psi C_\varphi - C_\psi S_\theta S_\varphi\right)\right\} + K_y Y_o = f_y \end{cases}$$

where $\bar{\bar{M}}$ is the total mass, i.e. it includes the mass of the drive system, the disc, and the effective mass of the vibrating structure.

In this investigation only the linearized versions of the set of Equations (12) will be studied. As suggested earlier in the Introduction, it is believed that in order for these devices to be useful in practice, the oscillations θ and φ should be reasonably small. Furthermore, the coordinate ψ will be dropped as a generalized coordinate and the spin velocity, $\dot{\psi}$, is assumed as a constant designated as Ω. Thus, the resulting equations are a set of coupled linear differential equations as shown below.

$$I_y \ddot{\theta} + (I_z - I_x)\Omega^2\theta + \Omega\dot{\varphi}(I_x + I_y - I_z) + K_\theta\theta + Mh(C_\psi \ddot{X}_0 + S_\psi \ddot{Y}_0) = 0$$

$$I_x \ddot{\varphi} + (I_z - I_y)\Omega^2\varphi - \Omega\dot{\theta}(I_x + I_y - I_z) + K_\phi\phi + Mh(S_\psi \ddot{X}_0 - C_\psi \ddot{Y}_0) = 0 \qquad (13)$$

$$\bar{M}\ddot{X}_0 + Mh\{C_\psi\ddot{\theta} + S_\psi\ddot{\phi} - \Omega^2(S_\psi\phi + C_\psi\theta) - 2S_\psi\Omega\dot{\theta} + 2C_\psi\Omega\dot{\varphi}\} + K_X X_0 = f_X$$

$$\bar{M}\ddot{Y}_0 + Mh\{S_\psi\ddot{\theta} - C_\psi\ddot{\phi} + \Omega^2(C_\psi\phi - S_\psi\theta) + 2C_\psi\Omega\dot{\theta} + 2S_\psi\Omega\dot{\varphi}\} + K_Y Y_0 = 0$$

The above set of equations, although simplified considerably from its original form (12), cannot be solved easily because of the periodic coefficients $\sin\psi$ and $\cos\psi$. Further simplification may, however, be accomplished by proper transformation of coordinates. Such a transformation may be defined as

$$\begin{aligned} \xi_1 &= S_\psi\theta \\ \xi_2 &= C_\psi\theta \\ \xi_3 &= S_\psi\varphi \\ \xi_4 &= C_\psi\varphi \end{aligned} \qquad (14)$$

The first of Equation (13) may be now multiplied by C_ψ and then by S_ψ to obtain

$$I_y(\ddot{\xi}_2 + 2\Omega\dot{\xi}_1 - \Omega^2\xi_2) + \Omega^2(I_z - I_x)\xi_2 + \Omega(I_x + I_y - I_z)(\dot{\xi}_4 + \Omega\xi_3) + Mh(C_\psi^2\ddot{X}_0 + S_\psi C_\psi \ddot{Y}_0) + K_\theta\xi_2 = 0 \qquad (15)$$

$$I_y(\ddot{\xi}_1 - 2\Omega\dot{\xi}_2 - \Omega^2\xi_1) + \Omega^2(I_z - I_x)\xi_1 + \Omega(I_x + I_y - I_z)(\dot{\xi}_3 - \Omega\xi_4) + Mh(S_\psi^2\ddot{Y}_0 + S_\psi C_\psi \ddot{X}_0) + K_\theta\xi_1 = 0 \qquad (16)$$

Similarly the two equations obtained from the second equation of (13) may be shown to be

$$I_x(\ddot{\xi}_4+2\Omega\dot{\xi}_3-\Omega^2\xi_4)+\Omega^2(I_z-I_y)\xi_4-\Omega(I_x+I_y-I_z)(\dot{\xi}_2+\Omega\xi_1)$$
$$+Mh(S_\psi C_\psi \ddot{X}_0-C_\psi^2\ddot{Y}_0)+K_\varphi\xi_4=0 \qquad (17)$$

$$I_x(\ddot{\xi}_3-2\Omega\dot{\xi}_4-\Omega^2\xi_3)+\Omega^2(I_z-I_y)\xi_3-\Omega(I_x+I_y-I_z)(\dot{\xi}_1-\Omega\xi_2)$$
$$+Mh(S_\psi^2\ddot{X}_0-S_\psi C_\psi\ddot{Y}_0)+K_\varphi\xi_3=0 \qquad (18)$$

Adding Equations (15) and (18) and subtracting Equation (16) from (17), the resulting equations may be shown to be

$$I_x\ddot{\eta}+\Omega I_z\dot{\zeta}+Mh\ddot{X}_0+K\eta=0 \qquad (19)$$

$$I_x\ddot{\zeta}-\Omega I_z\dot{\eta}+Mh\ddot{Y}_0+K\zeta=0 \qquad (20)$$

where the new coordinates η and ζ are defined by

$$\eta=\xi_2+\xi_3$$
$$\zeta=\xi_1-\xi_4 \qquad (21)$$

In deriving Equations (19) and (20), the inertias I_x and I_y have been assumed to be equal and the spring rates k_θ and k_φ have also been assumed to be the same, i.e. $k_\theta=k_\varphi=K$. Finally, the last two equations of (13) may be shown to reduce to

$$\bar{M}\ddot{X}_0+Mh\ddot{\eta}+K_x X_0=f_x \qquad (22)$$

$$\bar{M}\ddot{Y}_0+Mh\ddot{\zeta}+K_y Y_0=0 \qquad (23)$$

Thus, the simplified set of linearized governing equations of motion for the Perissogyro configuration A, may be written as

$$
\begin{aligned}
&\ddot{\eta} + \Omega \frac{I_z}{I_x} \dot{\zeta} + \frac{Mh}{I_x} \ddot{x}_0 + \frac{K}{I_x} \eta = 0 \\
&\ddot{\zeta} - \Omega \frac{I_z}{I_x} \dot{\eta} + \frac{Mh}{I_x} \ddot{y}_0 + \frac{K}{I_x} \zeta = 0 \\
&\ddot{\eta} + \frac{\bar{\bar{M}}}{Mh} \ddot{x}_0 + \frac{K_x}{Mh} x_0 = \frac{f_x}{Mh} \\
&\ddot{\zeta} + \frac{\bar{\bar{M}}}{Mh} \ddot{y}_0 + \frac{K_y}{Mh} y_0 = 0
\end{aligned}
\tag{24}
$$

Under steady-state conditions, the solutions for η, ζ x_0, y_0 may be assumed as

$$
\begin{aligned}
\eta &= \eta_0 e^{i\omega t} \\
\zeta &= \zeta_0 e^{i\omega t} \\
x_0 &= x_{0_1} e^{i\omega t} \\
y_0 &= y_{0_1} e^{i\omega t}
\end{aligned}
\tag{25}
$$

Substitution of the assumed form of solution in the set of Equations (24) yields the matrix equation

$$
\begin{bmatrix}
\frac{K}{I_x} - \omega^2 & i \frac{I_z}{I_x} \Omega\omega & -\frac{Mh\omega^2}{I_x} & 0 \\
-i \frac{I_z}{I_x} \Omega\omega & \frac{K}{I_x} - \omega^2 & 0 & -\frac{Mh\omega^2}{I_x} \\
-\omega^2 & 0 & \frac{K_x - \bar{\bar{M}}\omega^2}{Mh} & 0 \\
0 & -\omega^2 & 0 & \frac{K_y - \bar{\bar{M}}\omega^2}{Mh}
\end{bmatrix}
\begin{Bmatrix} \eta \\ \zeta \\ x_0 \\ y_0 \end{Bmatrix}
=
\begin{Bmatrix} 0 \\ 0 \\ \frac{f_x}{Mh} \\ 0 \end{Bmatrix}
\tag{26}
$$

From Equation (26), it is now possible to solve for the displacements in the X_f and Y_f directions for a given f_x. Also, the conditions necessary to obtain a null (zero displacement) in the X_f direction may be derived. Under these conditions, the effect in the Y_f direction may be determined.

Equation (26) may be written as

$$[D]\{q_i\} = \{f_i\} \tag{27}$$

where D is the coefficient matrix, q_i is the column matrix of the generalized coordinates and f_i, the column matrix of the generalized forces.

The natural frequencies for the system may be obtained by solving the characteristic equation $|D| = 0$ where $|D|$ represents the determinant of the coefficient matrix. Omitting the details of calculations, the expression for $|D|$ may be written as follows:

$$D = C_1\omega^8 + C_2\omega^6 + C_3\omega^4 + C_4\omega^2 + C_5$$

where

$$C_1 = -\left(\frac{Mh}{I_X} - \frac{\bar{\bar{M}}}{Mh}\right)^2$$

$$C_2 = -\left\{\left(\frac{Mh}{I_X} - \frac{\bar{\bar{M}}}{Mh}\right)\left(\frac{K_X + K_Y}{Mh} + \frac{2K\bar{\bar{M}}}{I_X Mh}\right) - \left(\frac{\Omega I_Z}{I_X}\frac{\bar{\bar{M}}}{Mh}\right)^2\right\}$$

$$C_3 = \left(\frac{K_X + K_Y}{Mh}\right)\left(\frac{KMh}{I_X^2} - \frac{\Omega^2 I_Z^2 \bar{\bar{M}}}{Mh\, I_X^2} - \frac{2K\bar{\bar{M}}}{I_X Mh}\right) - \frac{K_X K_Y}{M^2h^2} - \left(\frac{K\bar{\bar{M}}}{I_X Mh}\right)^2$$

$$C_4 = \frac{KK_Y}{I_X Mh}\left(\frac{2K_X}{Mh} - \frac{K\bar{\bar{M}}}{I_X Mh}\right) - \frac{K_X}{Mh}\left(\frac{K^2\bar{\bar{M}}}{I_X^2 Mh} + \frac{\Omega^2 I_Z^2 K_Y}{I_X^2 Mh}\right)$$

$$C_5 = -\frac{K^2}{I_X^2}\,\frac{K_X K_Y}{M^2h^2}$$

(29)

Similarly the expressions for X_o and Y_o may be shown to reduce to

$$\frac{DX_o}{f_o} = \omega^6\left(\frac{Mh}{I_X} - \frac{\bar{\bar{M}}}{Mh}\right) - \omega^4\left(\frac{KMh}{I_X^2} - 2\frac{K}{I_X}\frac{\bar{\bar{M}}}{Mh} - \Omega^2\frac{I_Z^2}{I_X^2}\frac{\bar{\bar{M}}}{Mh} - \frac{K_Y}{Mh}\right)$$
$$- \omega^2\left\{\frac{K^2}{I_X^2}\frac{\bar{\bar{M}}}{Mh} + \frac{K_Y}{Mh}\left(\Omega^2\frac{I_Z^2}{I_X^2} + \frac{2K}{I_X}\right)\right\} + \frac{K^2}{I_X^2}\frac{K_Y}{Mh} \qquad (30)$$

and

$$\frac{DY_o}{f_o} = \Omega\frac{I_Z}{I_X^2}Mh\omega^5 \qquad (31)$$

It may be noted from Equation (31) that the displacement along the Y direction can never be zero. Therefore, even though a null is attained along the X direction, the system may have oscillations in the orthogonal direction. This imposes a limitation on the usefulness of Perissogyro device. However, it is clear from Equation (31) that the displacement Y_o is linearly related to the speed of the gyro wheel. This property will be used later to discuss the development of the so-called Double Perisso.

Equation (30) when equated to zero represents the null equation for the system under consideration.

Equations (28), (30) and (31) are quite general in that they include the effects of spring rates in the pivots as well as along the X_f , Y_f directions. The solutions for these equations have been obtained with the aid of a digital computer. They can, however, be simplified considerably if the spring rates are assumed as zero and if $\bar{\bar{M}}=M$.

Thus, when $K=0=K_X=K_Y$, and $\bar{\bar{M}}=M$, the null equation is given by

$$\omega_n^2 = \frac{\Omega^2 I_Z^2}{I_X(I_X - Mh^2)} \qquad (32)$$

and the equation for the resonant frequencies may be shown to reduce to

$$\omega_r^2 = \frac{\Omega^2 I_Z^2}{(I_X - Mh^2)^2} \qquad (33)$$

Thus $$\left(\frac{\omega_n}{\omega_r}\right)^2 = 1 - \frac{Mh^2}{I_\chi} \tag{34}$$

i.e. $$\omega_\eta < \omega_r \tag{35}$$

An examination of Equation (32) indicates an interesting contrast with conventional absorbers in that the null frequency depends on the magnitude of the absorber mass.

Equations (30) and (32) indicate that the null frequency is related to the speed of the gyro wheel. Such relationships are characteristic of gyroscopic systems and provide the unique advantage by means of which the absorbers may be synchronized. Thus, with proper synchronization of the angular velocity of the gyro, the absorber will produce an antiresonance on the structure to which it is attached, at all values of the driving frequency. Details of such synchronization will be presented in the latter part of this report.

Numerical results obtained by solving the null and the characteristic equations for the single Perissogyro are presented graphically. Comparison has been made with the results obtained by experiment. A discussion of the results and conclusions will be postponed until after the analyses for the other configurations are presented.

The preceding analysis has shown that while the Perissogyro is capable of producing antiresonance in the direction of the forcing function, oscillations will always occur in the orthogonal direction. These oscillations may be of relatively small amplitude but they are nevertheless undesirable. As suggested earlier, the vibrations induced in the y direction are linearly related to the gyro angular velocity Ω. This leads one to believe that by superposing the effects of two Perissogyro vibration absorbers, the gyro angular velocities of which are opposite to one another ($\Omega_1 = -\Omega_2$), the effect in the y direction may altogether be eliminated. Such a device is designated here as "Double Perisso" and consists of a set of two Perissogyro vibration absorbers attached to the vibrating structure. The gyro wheel in one of the sets rotates in a direction opposite to that of the other, i.e. $\Omega_1 = -\Omega_2$. The analysis of such a combined system is presented below.

Since there are two absorbers attached together to the vibrating structure, there are, in general, six generalized coordinates, i.e. $\theta_1, \theta_2, \varphi_1, \varphi_2, x_0$ and y_0. It will be shown below that these reduce to three generalized coordinates when the two absorbers are identical in all respects.

From the analysis presented before, the governing equations may be written readily. Thus, the equations for the variables θ_i and φ_i are

$$I_y \ddot{\theta}_i + \Omega^2 \theta_i (I_z - I_x) + Mh(C_\psi \ddot{x}_0 \pm S_\psi \ddot{y}_0) \pm \Omega \dot{\varphi}_i (2I_x - I_z) + K\theta_i = 0$$

$$I_y \ddot{\varphi}_i + \Omega^2 \varphi_i (I_z - I_x) + Mh(\pm S_\psi \ddot{x}_0 - C_\psi \ddot{y}_0) \mp \Omega \dot{\theta}_i (2I_x - I_z) + K\varphi_i = 0 \qquad (36)$$

$i = 1, 2$

As before, in order to remove the periodic coefficient from the set of Equations (36), the θ_2 equation may be multiplied by C_ψ and the φ_2 equation by S_ψ. The resulting latter equation may be subtracted from the resulting former equation to obtain

$$I_y \ddot{\eta}_2 + I_z \Omega \dot{\xi}_2 + K\eta_2 + Mh\ddot{x}_0 = 0 \qquad (37)$$

Similarly, the θ_2 equation may be multiplied by S_ψ and the φ_2 equation by C_ψ. Addition of the resulting set of equations may be shown to reduce to

$$I_y \ddot{\xi}_2 - I_z \Omega \dot{\eta}_2 + K\xi_2 - Mh\ddot{y}_0 = 0 \qquad (38)$$

The following definitions of the new coordinates have been used in deriving the Equations (37) and (38)

$$\eta_2 = \xi_{22} - \xi_{32}$$
$$\xi_2 = \xi_{12} + \xi_{42} \qquad (39)$$

where

$$\xi_{12} = \theta_2 S_\psi$$
$$\xi_{22} = \theta_2 C_\psi$$
$$\xi_{32} = \varphi_2 S_\psi \qquad (40)$$
$$\xi_{42} = \varphi_2 C_\psi$$

The governing equations in the X_o, Y_o direction may be derived assuming that the forcing function f_x is equally shared by the two absorbers. Thus, in the X_o direction

$$\bar{M}\ddot{X}_o + Mh\ddot{\eta}_2 + K_X X_o = f_x/2$$

corresponding to the Equation (22) of the single Perissogyro, i.e.

$$\bar{M}\ddot{X}_o + Mh\ddot{\eta}_1 + K_X X_o = f_x/2$$

Addition of the above two equations yields

$$\bar{M}\ddot{X}_o + Mh(\ddot{\eta}_1+\ddot{\eta}_2) + 2K_X X_o = f_x \qquad (41)$$

In Equation (40) $\bar{M}$ includes the effective mass of the structure at the point of attachment, the mass of the two gyro discs and their drive systems. By a similar procedure, the equation in the Y_o direction may be reduced to

$$\bar{M}\ddot{Y}_o + Mh(\ddot{\zeta}_1-\ddot{\zeta}_2) + 2K_Y Y_o = 0 \qquad (42)$$

The governing equations for the double perisso may now be summarized as follows:

$$\begin{aligned}
&I_x\ddot{\eta}_1 + \Omega I_z\dot{\zeta}_1 + K\eta_1 + Mh\ddot{X}_o = 0\\
&I_x\ddot{\eta}_2 + \Omega I_z\dot{\zeta}_2 + K\eta_2 + Mh\ddot{X}_o = 0\\
&I_x\ddot{\zeta}_2 - \Omega I_z\dot{\eta}_2 + K\zeta_2 - Mh\ddot{Y}_o = 0\\
&I_x\ddot{\zeta}_1 - \Omega I_z\dot{\eta}_1 + K\zeta_1 + Mh\ddot{Y}_o = 0\\
&\bar{M}\ddot{X}_o + Mh(\ddot{\eta}_1+\ddot{\eta}_2) + 2K_X X_o = f_x\\
&\bar{M}\ddot{Y}_o + Mh(\ddot{\zeta}_1-\ddot{\zeta}_2) + 2K_Y Y_o = 0
\end{aligned} \qquad (43)$$

Assuming as before steady-state solutions for the variables $\eta_1, \eta_2, \zeta_1, \zeta_2, X_o$ and Y_o, the resulting equations in matrix form may be shown to be:

$$
\begin{bmatrix}
K - I_x\omega^2 & 0 & i I_z \Omega\omega & 0 & -Mh\omega^2 & 0 \\
0 & K - I_x\omega^2 & 0 & i I_z \Omega\omega & -Mh\omega^2 & 0 \\
-i I_z \Omega\omega & 0 & K - I_x\omega^2 & 0 & 0 & Mh\omega^2 \\
0 & -i I_z \Omega\omega & 0 & K - I_x\omega^2 & 0 & -Mh\omega^2 \\
0 & 0 & -Mh\omega^2 & Mh\omega^2 & 0 & 2K_y - \bar{M}\omega^2 \\
-Mh\omega^2 & -Mh\omega^2 & 0 & 0 & 2K_x - \bar{M}\omega^2 & 0
\end{bmatrix}
\begin{bmatrix} \eta_1 \\ \eta_2 \\ \zeta_1 \\ \zeta_2 \\ Y_0 \\ X_0 \end{bmatrix}
=
\begin{bmatrix} 0 \\ 0 \\ 0 \\ 0 \\ 0 \\ f_0 \end{bmatrix}
\tag{44}
$$

Computing γ_0 from the above matrix equation, it may be shown that γ_0 is identically zero. Using the fact that $\gamma_0 = 0$, the governing equations may be reduced to a simpler set as follows:

From the last equation of the set (43), $\zeta_1 = \zeta_2$. Then η_1 may be shown to be equal to η_2 from the third and fourth equations of (43). Then the set (43) reduces merely to

$$\begin{aligned} I_x \ddot{\eta} + \Omega I_z \dot{\zeta} + K\eta + Mh\ddot{X}_0 &= 0 \\ I_x \ddot{\zeta} - \Omega I_z \dot{\eta} + K\zeta &= 0 \\ \bar{M}\ddot{X}_0 + 2Mh\ddot{\eta} + 2K_x X_0 &= f_x \end{aligned} \tag{45}$$

As before, a steady-state solution yields the matrix equation (46), i.e.

$$\begin{bmatrix} K-\omega^2 I_x & i I_z \Omega \omega & -Mh\omega^2 \\ -i I_z \Omega \omega & K-\omega^2 I_x & 0 \\ -2Mh\omega^2 & 0 & 2K_x - \bar{M}\omega^2 \end{bmatrix} \begin{Bmatrix} \eta \\ \zeta \\ X_0 \end{Bmatrix} = \begin{Bmatrix} 0 \\ 0 \\ f_x \end{Bmatrix} \tag{46}$$

From the above equation X_0/f_x may be shown to be

$$\frac{X_0}{f_x} = \frac{(K-\omega^2 I_x)^2 - \Omega^2\omega^2 I_z^2}{(2K_x - \bar{M}\omega^2)\left\{(K-\omega^2 I_x)^2 - I_z^2\Omega^2\omega^2\right\} - 2M^2h^2\omega^4(K-\omega^2 I_x)} \tag{47}$$

from which the null equation may be readily written as

$$I_x^2\omega^4 - (2KI_x + \Omega^2 I_z^2)\omega^2 + K^2 = 0 \tag{48}$$

The null equation is independent of linear spring rates and mass ratio $\bar{M}$. The characteristic equation from which the natural frequencies for the system are computed may be shown to reduce to

$$\omega^6\left(2M^2h^2 I_x - \bar{M} I_x^2\right) + \omega^4\left(2K_x I_x^2 + 2K\bar{M} I_x + \bar{M} I_z^2\Omega^2 - 2KM^2h^2\right)$$

$$-\omega^2\left(\bar{M}K^2 + 4KK_x I_x + 2K_x I_z^2\Omega^2\right) + 2K^2K_x = 0 \tag{49}$$

Equations (48) and (49) reduce to very simple expressions if the spring rates are set to zero. Thus, the null and natural frequencies for the case when the spring rates are zero may be shown to be

$$\omega_\eta^2 = \Omega^2 \left(\frac{I_z}{I_x} \right)^2 \tag{50}$$

and

$$\omega_n^2 = \frac{\bar{M} I_z^2 \Omega^2}{I_x (\bar{M} I_x - 2M^2 h^2)} \tag{51}$$

If $\bar{M}$ is assumed simply as $2M$, further simplification results, i.e.

$$\omega_n^2 = \frac{I_z^2 \Omega^2}{I_x (I_x - Mh^2)} \tag{52}$$

Thus, for the special case (i.e. $\bar{M} = 2M$, $K = 0 = K_x$)

$$\left(\frac{\omega_\eta}{\omega_n} \right)^2 = 1 - \frac{Mh^2}{I_x} \tag{53}$$

This ratio is exactly the same as the ratio obtained for a single Perisso under the same assumptions.

It is observed that the null frequency equation for the single Perissogyro (for the special case) coincides with the characteristic equation for the corresponding double Perissogyro. A simple explanation for this coincidence may be offered as follows.

When the null frequency is attained in the single Perisso, displacement along X direction is zero, while the displacement along Y direction may take place. The force along X direction is reacted by the absorber, and $f_y = 0$.

When the double Perissogyro is oscillating at its natural frequency, the displacement along X direction is taking place, displacement along Y direction being always zero. The force along X direction is zero while f_y is being reacted by the absorber. Thus the governing equation should be the same since X and Y are interchangeable.

The coordinates η_1 and ζ_1 may also be obtained from Equation (46) in the form

$$\eta_1 = a e^{i\omega t} \quad , \quad \zeta_1 = i b e^{i\omega t}$$

where

$$D_1 a = Mh\omega^2 (K - I_x \omega^2)$$

$$D_1 b = I_x Mh\Omega\omega^3 \qquad (54)$$

D_1 in the above equation is given by the characteristic Equation (49).

Since

$$\eta_1 = \theta_1 C_\psi + \varphi_1 S_\psi$$
$$\zeta_1 = \theta_1 S_\psi - \varphi_1 C_\psi$$

then (55)

$$\theta_1 = \eta_1 C_\psi + \zeta_1 S_\psi$$
$$\varphi_1 = \eta_1 S_\psi - \zeta_1 C_\psi$$

and

i.e.

$$\theta_1 = e^{i\omega t}(a C_\psi + i b S_\psi)$$
$$\varphi_1 = e^{i\omega t}(a S_\psi - i b C_\psi) \qquad (56)$$

Using the trigomometric identities for C_ψ and S_ψ, θ_1 and φ_1 may be reduced to

$$\theta_1 = \left(\frac{a+b}{2}\right) e^{i(\omega+\Omega)t} + \left(\frac{a-b}{2}\right) e^{i(\omega-\Omega)t} \qquad (57)$$

$$i\varphi_1 = \left(\frac{a+b}{2}\right) e^{i(\omega+\Omega)t} - \left(\frac{a-b}{2}\right) e^{i(\omega-\Omega)t} \qquad (58)$$

As may be observed from Equations (57) and (58), two wave forms whose frequencies may differ considerably are superposed to obtain θ_1 and φ_1. Thus when the ratio $(\omega-\Omega)/(\omega+\Omega)$ is reasonably large, the so-called "beat phenomenon" results.

ALTERNATE CONFIGURATION OF THE

"PERISSOGYRO VIBRATION ABSORBER"

Figure 2 shows schematically the configuration whose analysis is presented below. The gyro disc in this case rotates relative to the shaft on which it is mounted so that the Ω vector is now situated along the shaft perpendicular to the plane of the gyro wheel. The shaft itself is mounted on a cross pivot so that the device may oscillate in two directions perpendicular to each other. The motion of this configuration resembles, in many respects, the motion of tops.

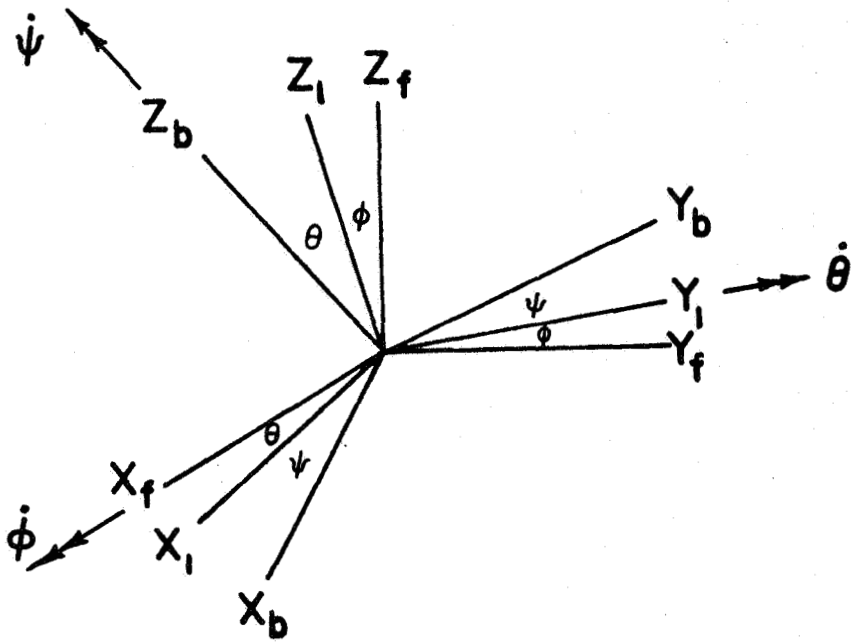

Figure 5. Coordinate Transformation

As before, the final position of a mass element situated on the gyro wheel may be obtained by successive Euler-type rotations given in the following sequence: rotation φ about X_f, rotation θ about Y_1 (i.e. rotated Y axis) and rotation ψ about Z_b (i.e. rotated Z axis). The fixed system of coordinates X_f, Y_f, Z_f can translate in the X_f and Y_f directions. The directions of the cross pivots coincide with the X_f and Y_f directions. The centroid of the spinning body may be assumed to be located at h units from the origin O.

The matrices which transform the coordinates of a mass element from the body axes into those referred to the fixed axes may be represented by Φ, Θ and Ψ so that

$$\begin{Bmatrix} X_f \\ Y_f \\ Z_f \end{Bmatrix} = [\Phi][\Theta][\Psi] \begin{Bmatrix} X_b \\ Y_b \\ Z_b \end{Bmatrix} \tag{59}$$

where

$$\Phi = \begin{pmatrix} 1 & 0 & 0 \\ 0 & C_\varphi & -S_\varphi \\ 0 & S_\varphi & C_\varphi \end{pmatrix}$$

$$\Theta = \begin{pmatrix} C_\theta & 0 & S_\theta \\ 0 & 1 & 0 \\ -S_\theta & 0 & C_\theta \end{pmatrix}$$

$$\Psi = \begin{pmatrix} C_\psi & -S_\psi & 0 \\ S_\psi & C_\psi & 0 \\ 0 & 0 & 1 \end{pmatrix} \tag{60}$$

and φ, θ, ψ are rotations about X_f, Y_1, Z_b axes as shown in Figure 5.

Upon multiplication of the matrices $\Phi\,\Theta\,\Psi$, X_f, Y_f and Z_f may be shown to be

$$\begin{aligned} X_f &= X_o + C_\psi C_\theta X_b - S_\psi C_\theta Y_b + S_\theta Z_b \\ Y_f &= Y_o + (S_\psi C_\varphi + C_\psi S_\theta S_\varphi) X_b + (C_\psi C_\varphi - S_\psi S_\theta S_\varphi) Y_b - C_\theta S_\varphi Z_b \\ Z_f &= (S_\psi S_\varphi - C_\psi C_\varphi S_\theta) X_b + (C_\psi S_\varphi + S_\psi S_\theta C_\varphi) Y_b + C_\theta C_\varphi Z_b \end{aligned} \tag{61}$$

with the same notations as before.

As before, the procedure would consist of computing $\dot{X}_f, \dot{Y}_f, \dot{Z}_f$ to derive an expression for the total kinetic energy T. Omitting all the intermediate calculations, may be shown to reduce to:

$$T = \frac{\bar{M}}{2}\left(\dot{X}_0^2 + \dot{Y}_0^2\right) + \frac{1}{2} I_Z \dot{\psi}^2 + \frac{1}{2} I_X \dot{\theta}^2 + \frac{1}{2}\left(S_\theta^2 I_Z + C_\theta^2 I_X\right)\dot{\varphi}^2$$
$$+ S_\theta I_Z \dot{\psi}\dot{\varphi} + Mh\left(C_\theta \dot{\theta}\dot{X}_0 - C_\theta C_\varphi \dot{\varphi}\dot{Y}_0 + S_\theta S_\varphi \dot{\theta}\dot{Y}_0\right) \tag{62}$$

and the potential energy V may be written as

$$V = \frac{1}{2}\left(K_\theta \theta^2 + K_\varphi \varphi^2 + K_X X_0^2 + K_Y Y_0^2\right) \tag{63}$$

In the above computations, symmetry of the spinning body is assumed to exist so that the product of inertia terms are set to zero. Also, the moments of inertia I_Z, I_X are referred to the axes passing through the origin O.

The governing equations of motion for the configuration may now be written by forming the Lagrangian function T-V. Again omitting all the details of calculations, the equations of motion may be shown to be:

$$\ddot{\psi} + \left(\ddot{\varphi} S_\theta + C_\theta \dot{\theta}\dot{\varphi}\right) = 0$$
$$I_X \ddot{\theta} + Mh\left(C_\theta \ddot{X}_0 + S_\theta S_\varphi \ddot{Y}_0\right) + \left(I_Y - I_Z\right) S_\theta C_\theta \dot{\varphi}^2 - C_\theta I_Z \dot{\psi}\dot{\varphi} + K_\theta \theta = 0$$
$$\left(I_Z S_\theta^2 + I_Y C_\theta^2\right)\ddot{\varphi} + 2\left(I_Z - I_Y\right) S_\theta C_\theta \dot{\varphi}\dot{\theta} + S_\theta I_Z \ddot{\psi} + C_\theta I_Z \dot{\psi}\dot{\theta} - Mh C_\theta C_\varphi \ddot{Y}_0 + K_\varphi \varphi =$$
$$\bar{M}\ddot{X}_0 + Mh\left(C_\theta \ddot{\theta} - S_\theta \dot{\theta}^2\right) + K_X X_0 = f_X$$
$$\bar{M}\ddot{Y}_0 + Mh\left\{S_\theta S_\varphi \ddot{\theta} - C_\theta C_\varphi \ddot{\varphi} + C_\theta S_\varphi\left(\dot{\varphi}^2 + \dot{\theta}^2\right) + 2 S_\theta C_\varphi \dot{\varphi}\dot{\theta}\right\} + K_Y Y_0 = 0$$

(64)

The first equation in the above set may be written as:

$$\frac{d}{dt}\left(\dot{\psi} + S_\theta \dot{\varphi}\right) = 0 \tag{65}$$

Therefore $\dot{\psi} + s_\theta \dot{\varphi}$ is a constant, i.e. the total angular velocity component along the body centerline does not change during the motion. This condition may be considered as an initial condition for the motion.

In order to obtain solutions, as before, θ and φ may be assumed as small. With $\dot{\psi} = \Omega$, the linearized equations of motion may be written as:

$$
\begin{aligned}
I_x \ddot{\theta} - I_z \Omega \dot{\varphi} + Mh \ddot{x}_0 + K_\theta \theta &= 0 \\
I_y \ddot{\varphi} + I_z \Omega \dot{\theta} - Mh \ddot{y}_0 + K_\varphi \varphi &= 0 \\
\bar{M} \ddot{x}_0 + Mh \ddot{\theta} + K_x x_0 &= f_x \\
\bar{M} \ddot{y}_0 - Mh \ddot{\varphi} + K_y y_0 &= 0
\end{aligned}
\qquad (66)
$$

It may be noted that θ, φ, x_0 and y_0 themselves serve as generalized coordinates so that no transformation of the nature used before in the Perissogyro vibration absorber is necessary. Clearly, such a simplification is the direct result of the cross pivots being fixed in the x_f, y_f and z_f system.

As before, assuming steady-state solutions $\theta = \theta_0 e^{i\omega t}$, $\varphi = \varphi_0 e^{i\omega t}$, $x_0 = x_{0_1} e^{i\omega t}$, $y_0 = y_{0_1} e^{i\omega t}$, and $f_x = f_0 e^{i\omega t}$, the null equation and the characteristic equation may be obtained. Thus

$$
\begin{bmatrix}
K_\theta - I_x\omega^2 & -i I_z \Omega \omega & -Mh\omega^2 & 0 \\
i I_z \Omega \omega & K_\varphi - I_x \omega^2 & 0 & -Mh\omega^2 \\
0 & -Mh\omega^2 & 0 & K_y - \bar{M}\omega^2 \\
-Mh\omega^2 & 0 & K_x - \bar{M}\omega^2 & 0
\end{bmatrix}
\begin{bmatrix} \theta \\ \varphi \\ y_0 \\ x_0 \end{bmatrix}
=
\begin{bmatrix} 0 \\ 0 \\ 0 \\ f_x \end{bmatrix}
\qquad (67)
$$

From Equation (67), $\mathcal{D}\chi_0/f_0$ may be shown to be ($\mathcal{D}$ is the determinant of the coefficient matrix):

$$\frac{\mathcal{D}\chi_0}{f_0} = (K_\theta - \omega^2 I_x)\left\{(\bar{\bar{M}}\omega^2 - K_y)(K_\varphi - \omega^2 I_x) + M^2h^2\omega^4\right\} - (\bar{\bar{M}}\omega^2 - K_y) I_z^2 \Omega^2 \omega^2 \tag{68}$$

Thus, the null equation when the spring rates K_θ, K_φ and K_y are identically zero may be shown to reduce to:

$$\omega_\eta = \frac{\Omega I_z}{\sqrt{I_x\left(I_x - \frac{M^2h^2}{\bar{\bar{M}}}\right)}} \tag{69}$$

Similarly, the characteristic equation may be obtained by letting $\mathcal{D} = 0$, i.e.

$$-(K_\theta - I_x\omega^2)(K_\varphi - I_x\omega^2)(K_y - \bar{\bar{M}}\omega^2)(K_x - \bar{\bar{M}}\omega^2) +$$
$$(K_\theta - I_x\omega^2)(K_x - \bar{\bar{M}}\omega^2) M^2h^2\omega^4 + (K_x - \bar{\bar{M}}\omega^2)(K_y - \bar{\bar{M}}\omega^2) I_z^2\Omega^2\omega^2$$
$$+ (K_\varphi - I_x\omega^2)(K_y - \bar{\bar{M}}\omega^2) M^2h^2\omega^4 - M^4h^4\omega^8 = 0 \tag{70}$$

Setting all the spring rates to zero, Equation (70) may be simplified as

$$\omega_\pi = \frac{\Omega I_z}{I_x - \frac{M^2h^2}{\bar{\bar{M}}}} \tag{71}$$

so that the ratio

$$\frac{\omega_\eta}{\omega_\pi} = \sqrt{1 - \frac{M^2h^2}{\bar{\bar{M}} I_x}} \tag{72}$$

i.e. $\omega_\eta < \omega_\xi$

An examination of Figure 4 indicates that the generalized coordinates η, ξ for the Perissogyro are written in terms of the angular oscillations θ, φ in the rotating system of coordinates. Since the pivots in the configuration shown in Figure 2 do not rotate, θ and φ themselves serve as generalized coordinates in this case. Thus, the equations of motion are very similar to Equation (24) and the null Equation (69) for this configuration coincides with Equation (32) of the Perissogyro. By virtue of the transformation Equation (21), the angular oscillatory responses in the two devices will, however, be different. In terms of null characteristics, the configuration shown in Figure 2 is identical to that of Figure 1. Therefore, further discussion will be confined to the Perissogyro vibration absorber only.

CORIOLIS VIBRATION ABSORBER

The analysis presented below pertains to the configuration shown in Figure 3. Two inertial elements are arranged in such a manner that their pivotal axes are at right angles to each other. As in the case of the configuration shown in Figure 1, the entire system rotates in unison. The device is designated as "Coriolis Vibration Absorber". It is evident that the governing equations of motion for the Coriolis Vibration Absorber can be obtained directly from those of the "Perissogyro Vibration Absorber", with minor modifications. Since the latter represents the case of an inertial element which can have angular oscillations about two axes, it is only necessary to suppress one of these freedoms of angular oscillations, in order to describe one element of the Coriolis absorber. Thus for each element, the governing linear equations of motion can be written directly from the set of Equations (12) as follows:

$$I_{g_i}\ddot{\theta}_i + \Omega^2\left(I_{z_i} - I_{x_i}\right)\theta_i + M_i h_i C_{\psi_i}\ddot{X}_o + M_i h_i S_{\psi_i}\ddot{Y}_o + K_i\theta_i = 0 \qquad i = 1, 2 \cdots n \tag{73}$$

where θ_i represents the amplitude of angular oscillation of the inertial element. In the above equation, the coordinates X_o, Y_o represent as before, the amplitude of vibrations along the X_f and Y_f axes and are common to the entire system.

Similarly the equations of motion corresponding to the coordinates X_o and Y_o for each element, may be written as

$$\bar{\bar{M}}_i\ddot{X}_o + M_i h_i C_{\psi_i}\ddot{\theta}_i - \Omega^2 M_i h_i C_{\psi_i}\theta_i - 2\Omega M_i h_i S_{\psi_i}\dot{\theta}_i + K_{x_i}X_o = f_{x_i} \tag{74}$$

and

$$\bar{\bar{M}}\ddot{Y}_o + M_i h_i S_{\psi_i}\ddot{\theta}_i - \Omega^2 M_i h_i S_{\psi_i}\theta_i + 2\Omega M_i h_i C_{\psi}\dot{\theta}_i + K_{y_i}Y_o = 0 \tag{75}$$

where $f_{x_i} = \frac{f_x}{n}$, $K_{y_i} = \frac{K_y}{n}$, $K_{x_i} = \frac{K_x}{n}$

Equations (74) and (75) for each element may be combined in the following manner to represent all the elements, i.e.,

$$\left(\bar{\bar{M}}_1 + \bar{\bar{M}}_2 + \cdots\right)\ddot{X}_o + \left(M_1 h_1 C_{\psi_1}\ddot{\theta}_1 + M_2 h_2 C_{\psi_2}\ddot{\theta}_2 + \cdots\right)$$
$$- \Omega^2\left(M_1 h_1 C_{\psi_1}\theta_1 + M_2 h_2 C_{\psi_2}\theta_2 + \cdots\right) - 2\Omega\left(M_1 h_1 S_{\psi_1}\dot{\theta}_1 + M_2 h_2 S_{\psi_2}\dot{\theta}_2 + \cdots\right) \tag{76}$$
$$+ K_x X_o = f_x$$

and

$$(\bar{\bar{M}}_1+\bar{\bar{M}}_2+\cdots)\,\ddot{Y}_0 + (M_1 h_1 S_{\psi_1}\ddot{\theta}_1 + M_2 h_2 S_{\psi_2}\ddot{\theta}_2+\cdots) - \Omega^2(M_1 h_1 S_{\psi_1}\theta_1 + M_2 h_2 S_{\psi_2}\theta_2+\cdots)$$

$$+ 2\Omega\,(M_1 h_1 C_{\psi_1}\dot{\theta}_1 + M_2 h_2 C_{\psi_2}\dot{\theta}_2+\cdots) + K_Y Y_0 = 0$$

(77)

As before, in order to reduce the governing equations of motion into a set of linear differential equations with constant coefficients, each of the set of Equations (73) is multiplied by S_{ψ_i} ; and the resulting set is added to obtain

$$(I_{Y_1} S_{\psi_1}\ddot{\theta}_1 + I_{Y_2} S_{\psi_2}\ddot{\theta}_2+\cdots) + \Omega^2\{(I_{Z_1}-I_{X_1})S_{\psi_1}\theta_1 + (I_{Z_2}-I_{X_2})S_{\psi_2}\theta_2+\cdots\} +$$

$$(M_1 h_1 S_{\psi_1} C_{\psi_1} + M_2 h_2 S_{\psi_2} C_{\psi_2}+\cdots)\,\ddot{X}_0 + (M_1 h_1 S_{\psi_1} C_{\psi_1} + M_2 h_2 S_{\psi_2} C_{\psi_2}+\cdots)\,\ddot{Y}_0$$

$$+ (K_1 C_{\psi_1}\theta_1 + K_2 C_{\psi_2}\theta_2+\cdots) = 0$$

(78)

A similar equation is obtained by multiplying Equation (73) by and adding the resulting set to obtain

$$(I_{Y_1} C_{\psi_1}\ddot{\theta}_1 + I_{Y_2} C_{\psi_2}\ddot{\theta}_2+\cdots) + \Omega^2\{(I_{Z_1}-I_{X_1})C_{\psi_1}\theta_1 + (I_{Z_2}-I_{X_2})C_{\psi_2}\theta_2+\cdots\} +$$

$$+(M_1 h_1 C_{\psi_1}^2 + M_2 h_2 C_{\psi_2}^2+\cdots)\,\ddot{X}_0 + (M_1 h_1 S_{\psi_1} C_{\psi_1} + M_2 h_2 S_{\psi_2} C_{\psi_2}+\cdots)\,\ddot{Y}_0$$

$$+ (K_1 C_{\psi_1}\theta_1 + K_2 C_{\psi_2}\theta_2+\cdots) = 0$$

(79)

Equations (76), (77), (78) and (79) represent the governing equations of motion for n inertial elements connected together at a common location on a vibrating structure. $\psi_1, \psi_2 \cdots$ define the relative orientations of the elements at all times.

The periodic coefficients in the above set of equations may be removed by suitable transformation of coordinates. Such a transformation is shown below:

$$\xi_1 = \theta_1 S_{\psi_1} + \theta_2 S_{\psi_2} + \cdots$$

$$\xi_2 = \theta_1 C_{\psi_1} + \theta_2 C_{\psi_2} + \cdots$$

(80)

Omitting the details of algebraic manipulation, Equations (78) and (79) may be written in terms of the transformed generalized coordinates ξ_1, ξ_2 and X_0, Y_0 as follows. In the following $M_1 = M_2 = \cdots = M$ and $h_1 = h_2 = \cdots = h$ and $K_1 = K_2 = \cdots = K$, $I_{Y_1} = I_{Y_2} = \cdots$, $I_{X_1} = I_{X_2} = \cdots$

$$I_y\left(\ddot{\xi}_1 - 2\Omega\dot{\xi}_2 - \Omega^2\xi_1\right) + \Omega^2\left(I_z - I_x\right)\xi_1 + Mh\left(S_{\psi_1}C_{\psi_1} + S_{\psi_2}C_{\psi_2} + \cdots\right)\ddot{X}_0$$

$$+ Mh\left(S^2_{\psi_1} + S^2_{\psi_2} + \cdots\right)\ddot{Y}_0 + K\xi_1 = 0 \tag{81}$$

and

$$I_y\left(\ddot{\xi}_2 + 2\Omega\dot{\xi}_1 - \Omega^2\xi_2\right) + \Omega^2\left(I_z - I_x\right)\xi_2 + Mh\left(C^2_{\psi_1} + C^2_{\psi_2} + \cdots\right)\ddot{X}_0$$

$$+ Mh\left(S_{\psi_1}C_{\psi_1} + S_{\psi_2}C_{\psi_2} + \cdots\right)\ddot{Y}_0 + K\xi_2 = 0 \tag{82}$$

Considering only two inertial elements, as shown in Figure 3, $\psi_1 = \psi$ and $\psi_2 = \psi + \pi/2$. With these values for ψ_1 and ψ_2 Equations (81) and (82) reduce to

$$I_y\left(\ddot{\xi}_1 - 2\Omega\dot{\xi}_2 - \Omega^2\xi_1\right) + \Omega^2\left(I_z - I_x\right)\xi_1 + Mh\ddot{Y}_0 + K\xi_1 = 0 \tag{83}$$

$$I_y\left(\ddot{\xi}_2 + 2\Omega\dot{\xi}_1 - \Omega^2\xi_2\right) + \Omega^2\left(I_z - I_x\right)\xi_2 + Mh\ddot{X}_0 + K\xi_2 = 0 \tag{84}$$

Similarly, Equations (76) and (77) reduce to

$$\bar{M}\ddot{X}_0 + Mh\ddot{\xi}_2 + K_X X_0 = f_X \tag{85}$$

and

$$\bar{M}\ddot{Y}_0 + Mh\ddot{\xi}_1 + K_Y Y_0 = 0 \tag{86}$$

Assuming steady-state oscillations, the null and characteristic equations are derived in a manner similar to that shown for the "Perissogyro Vibration Absorber" and are presented below.

The equation that determines the null frequencies for the Coriolis absorber is

$$\omega^6 \{ I_y (\bar{M} I_y - M_1^2 h_1^2) \} +$$

$$\omega^4 \left[M_1^2 h_1^2 (K_T + I\Omega^2) - K_y I_y^2 - 2\bar{M} I_y \{ K_T + \Omega^2 (I_z - I_x + I_y) \} \right] +$$

$$\omega^2 \left[\bar{M} (K_T + I\Omega^2)^2 + 2 K_y I_y \{ (I_z - I_x + I_y) \Omega^2 + K_T \} \right] -$$

$$\{ K_y (I\Omega^2 + K_T)^2 \} = 0 ;$$

$$I = I_z - I_x - I_y$$

(87)

and the equation that determines the natural frequencies is

$$\omega^8 (\bar{M} I_y - M_1^2 h_1^2)^2 - \omega^6 \{ (K_x + K_y) I_y (\bar{M} I_y - M_1^2 h_1^2) -$$

$$2 I \bar{M} M_1^2 h_1^2 \Omega^2 + 2 K_T (M^2 I_y - \bar{M} M_1^2 h_1^2) + 2 I_y (I_z - I_x + I_y) \bar{M}^2 \Omega^2 \}$$

(88)

$$+ \omega^4 \left[(K_x + K_y) \{ (K_T + I\Omega^2)(M_1^2 h_1^2 - 2\bar{M} I_y) - 4 \bar{M} I_y^2 \Omega^2 \} \right.$$

$$\left. - \bar{M}^2 (K_T + I\Omega^2)^2 \right] + \omega^2 \left[\bar{M} (K_x + K_y)(K_T + I\Omega^2)^2 + \right.$$

$$\left. 2 K_x K_y I_y \{ K_T + (I_z - I_x + I_y) \Omega^2 \} \right] - K_x K_y (K_T + I\Omega^2)^2 = 0$$

EXPERIMENTAL SETUP AND PROCEDURES

The overall purpose of the experimentation was to obtain reasonable confirmation of the theoretical development of the Perissogyro Vibration Absorber. In order to accomplish this, an absorber was designed using a Hooke's Joint, one end of which is connected to a synchronous motor and the other to a circular aluminum plate at one end of a steel rod. Details such as the weights, dimensions, etc. of the single Perissogyro are listed in Table 1. The schematic and a photograph of the setup are shown in Figures 6 and 7. The speed (rpm) and the direction of rotation of the motor could be controlled at either 1800 rpm or 3600 rpm. The entire absorber was then mounted on two shafts which rotate in opposite directions in order to remove the effect of friction forces along the direction of oscillation. Plunger springs were mounted laterally to provide lateral spring rate.

A 50-pound shaker was used to excite the system. Two MB velocity pickups were mounted on the base of the Perissogyro in the direction of excitation and perpendicular to it. The outputs of the pickups were fed to an oscilloscope from which the results were recorded manually. On some tests, actual traces of the output were obtained to facilitate discussion of results.

In order to compare the theoretical results with the experimental results, it was necessary to determine the actual spring rate in the lateral direction. This was measured by means of a simple experiment, the results of which are shown in Figure 8. This load-displacement curve being slightly nonlinear, the spring rate was approximated to be around 600 pounds/inch.

In order to experimentally determine the variation of antiresonant frequency with the speed of the gyro wheel, the excitation frequency was set at a particular value and the motor running at 3600 rpm was turned off. As the motor continued to decelerate, the actual instantaneous rpm was read on an electronic counter when the null was located on the oscilloscope. This procedure was repeated for various values of the excitation frequency. A comparison of the null-rpm characteristics predicted by theory (with K_y as parameter) with those obtained from experiment is presented in Figure 9. It may be noted that the latter results approximate closely to the former at $K_y = 600$ #/inch .

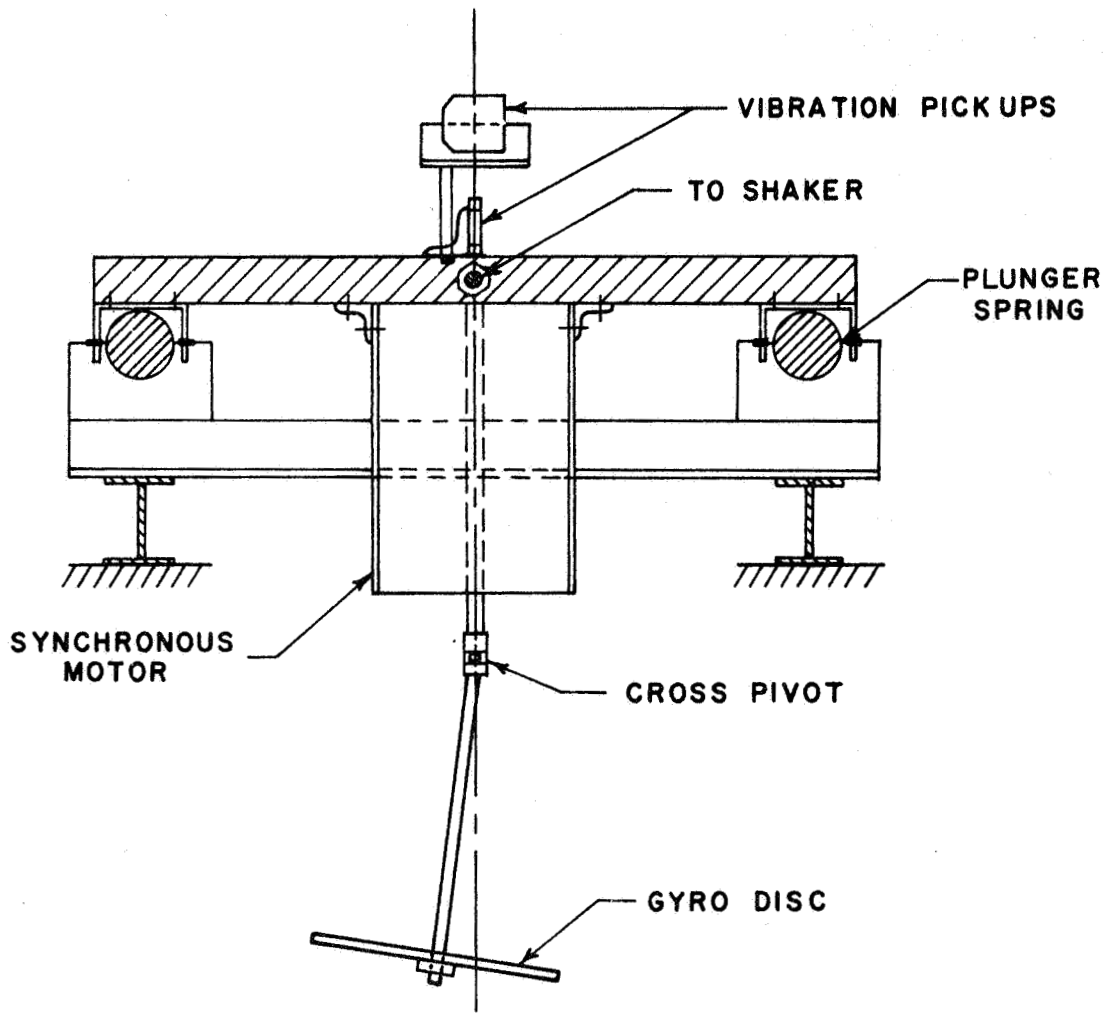

Figure 6. Schematic of the Experimental Setup

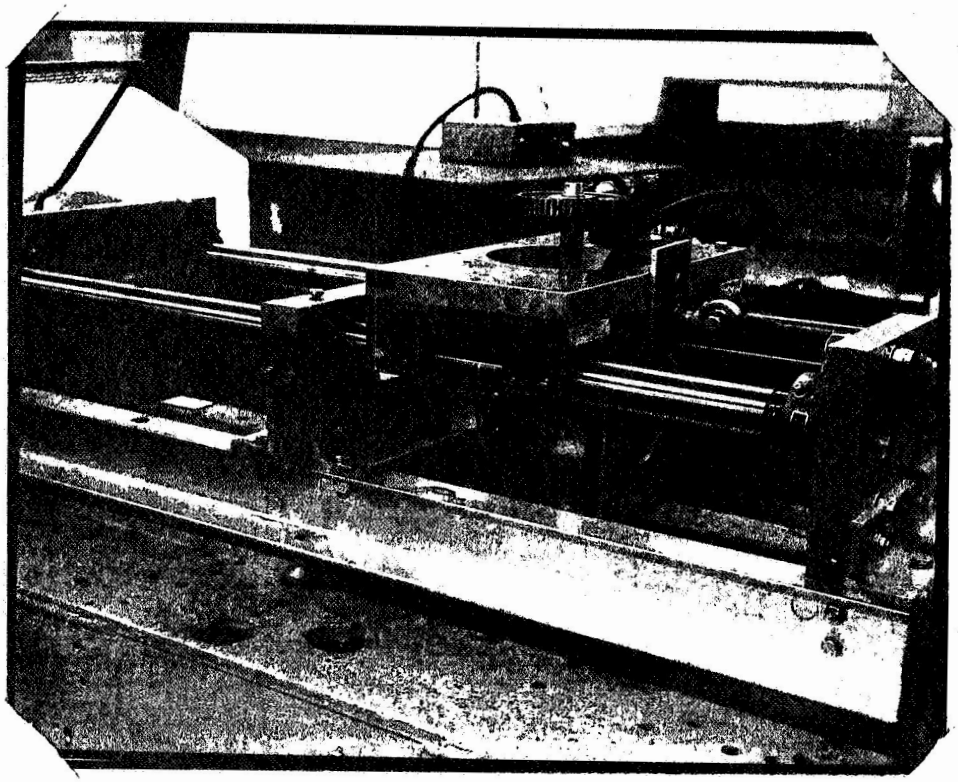

Figure 7. Photograph of the Experimental Setup of the Perissogyro Vibration Absorber

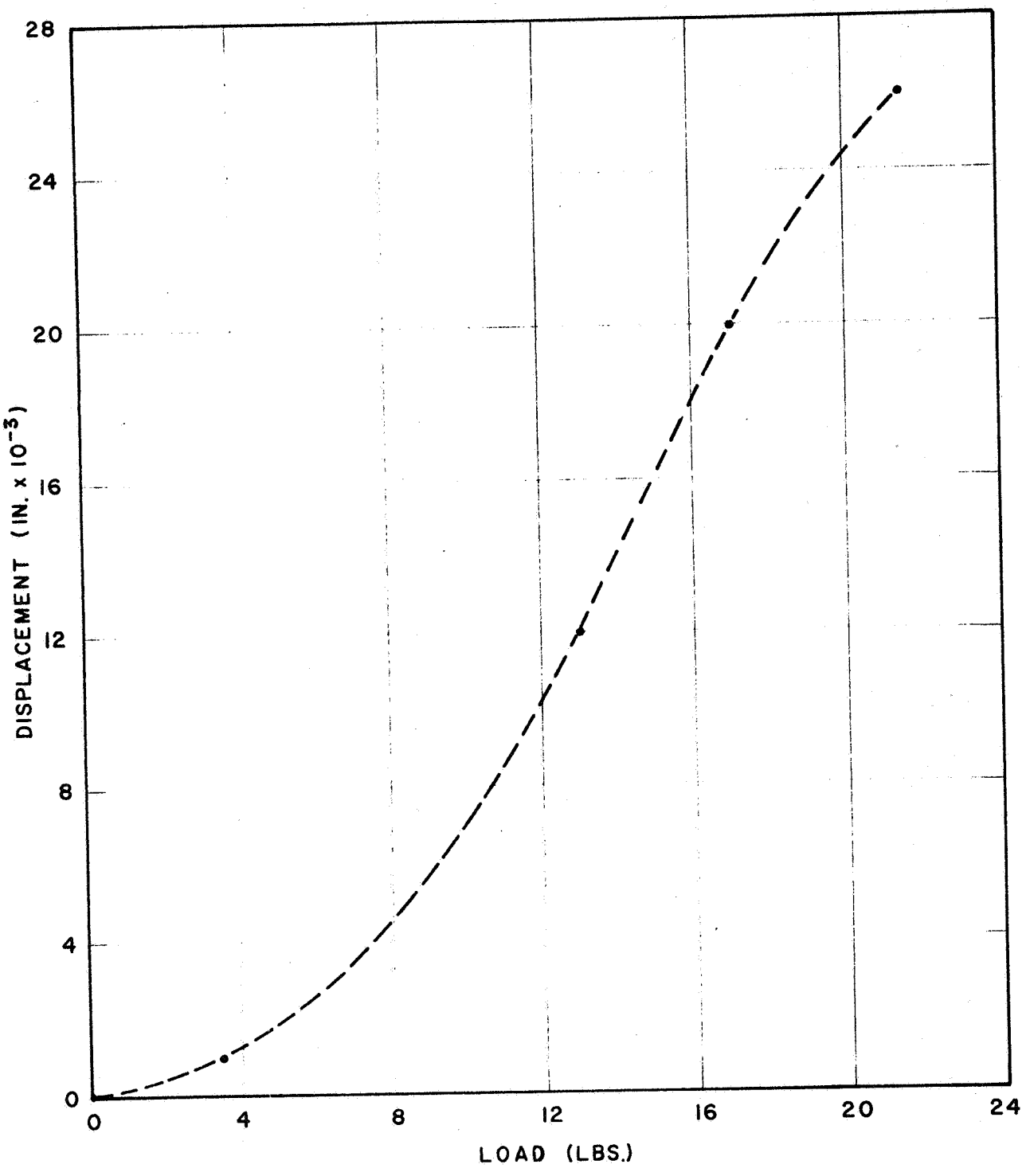

Figure 8. Determination of the Lateral Spring Rate

One of the problems that was encountered during experimentation pertains to self-excited oscillations of the Perissogyro. These oscillations were at times quite violent and repeated trials were necessary before reasonably satisfactory conditions were obtained. The linear theory does not suggest possibilities of any such apparently unstable conditions. Further detailed experimental and theoretical investigations would be necessary to obtain a fully satisfactory explanation of this problem.

The photograph of the setup for testing the double Perissogyro vibration absorber is shown in Figure 10. Two single Perissogyros are mounted side by side and rigidly connected together by means of a connecting plate. The experimental procedures were similar to those adopted in the tests on single Perissogyro vibration absorber.

Preliminary tests were performed using the same dimensions as those of the single Perissogyro device. This resulted in self-excited oscillations of the gyro disc, which were considered unsatisfactory to obtain reasonable data. The length of the shaft was reduced and the aluminum gyro disc was replaced by a steel plate. The details of the double Perissogyro including the weights, etc. are tabulated in Table 2. These modifications improved the conditions considerably, and therefore, the data presented here were obtained for the double Perissogyro configuration whose dimensions are as shown in Table 2.

A major problem that was encountered during the tests on the double Perissogyro was that of an angular oscillation of the entire device about a vertical axis of symmetry. Thus, part of the energy was transferred to this rotational motion. It may be recalled that in the theoretical analysis, this additional degree of freedom has not been considered. The experimental data seems to be considerably influenced by this undesirable oscillation. Preliminary attempts to overcome this phenomenon have failed. This phenomenon resulted in producing beats so that a rather laborious data reduction was necessary to obtain the amplitudes and frequencies of oscillation of the double Perissogyro.

Some of the traces obtained during the tests are presented in Figures 11 and 12. Because of the presence of angular oscillations about a vertical axis referred to earlier, null-rpm characteristics of the double Perissogyro could not be obtained.

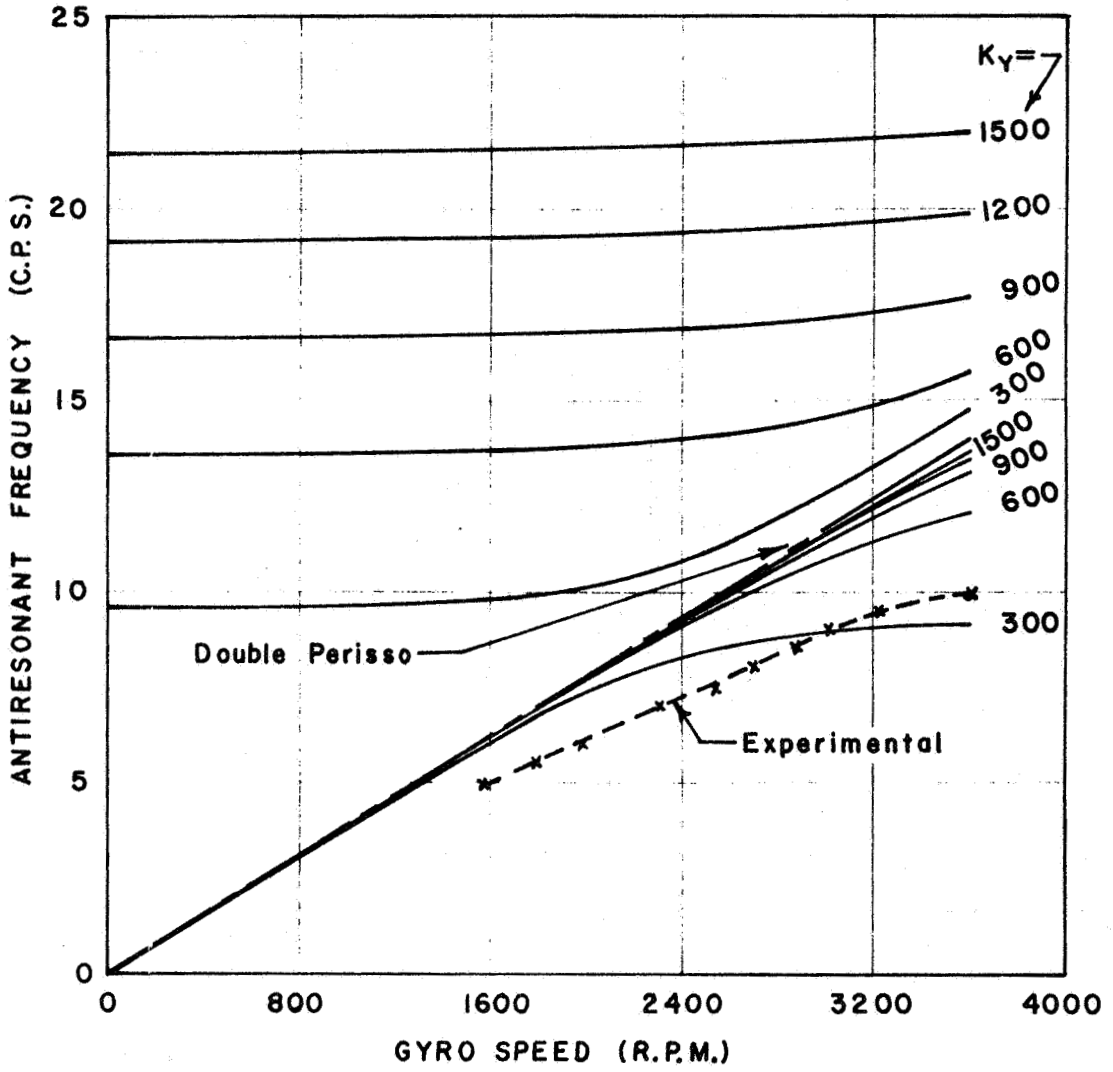

Figure 9. Null-Rpm Characteristics of Perissogyro Vibration Absorbers

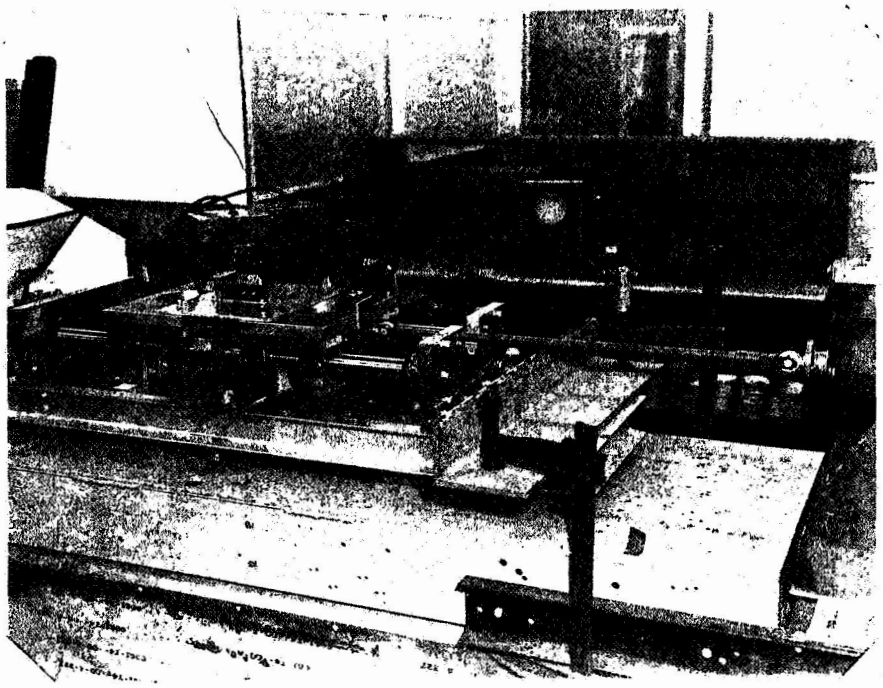

Figure 10. Photograph of the Experimental Setup of the Double Perissogyro Vibration Absorber

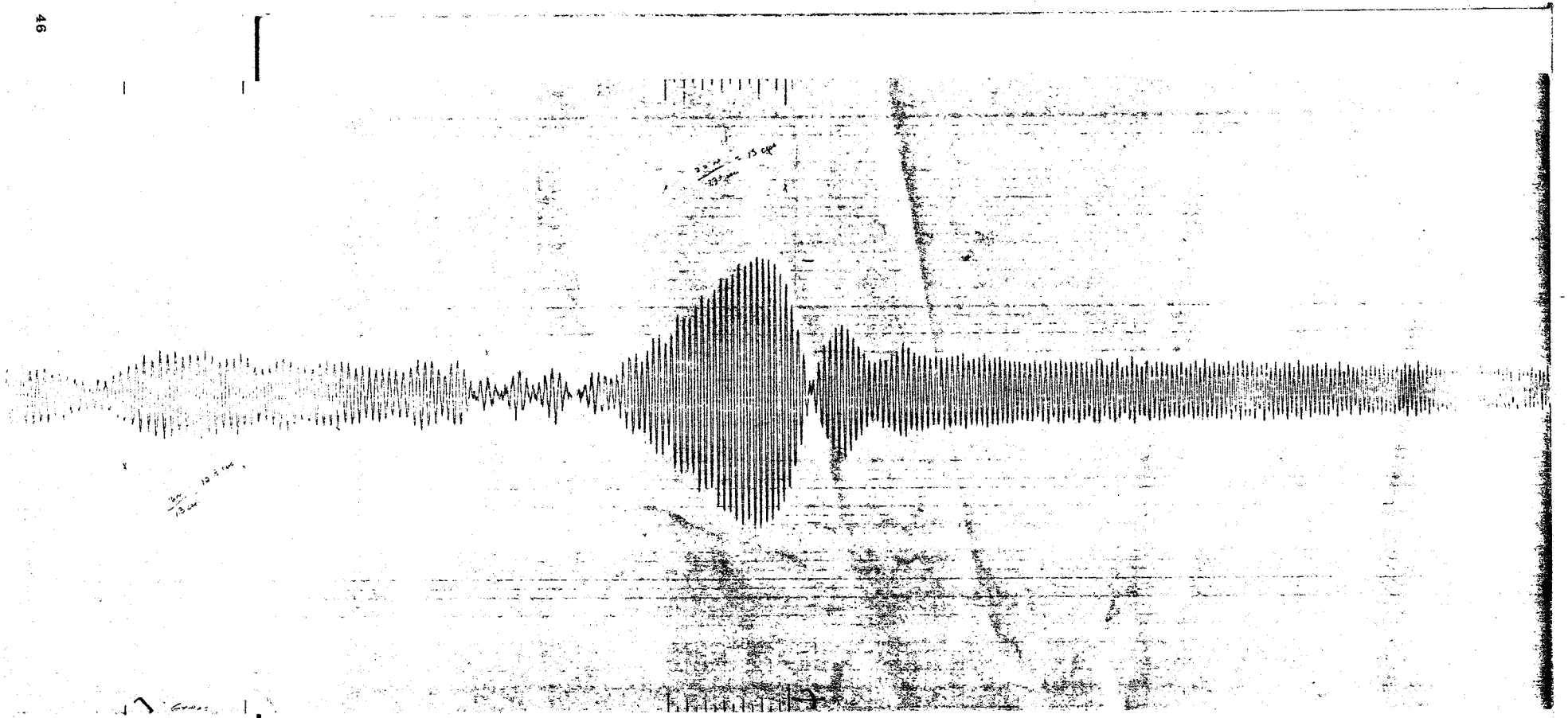

Figure 11. Example of Traces Obtained by Experiment on Double Perissogyro Absorber

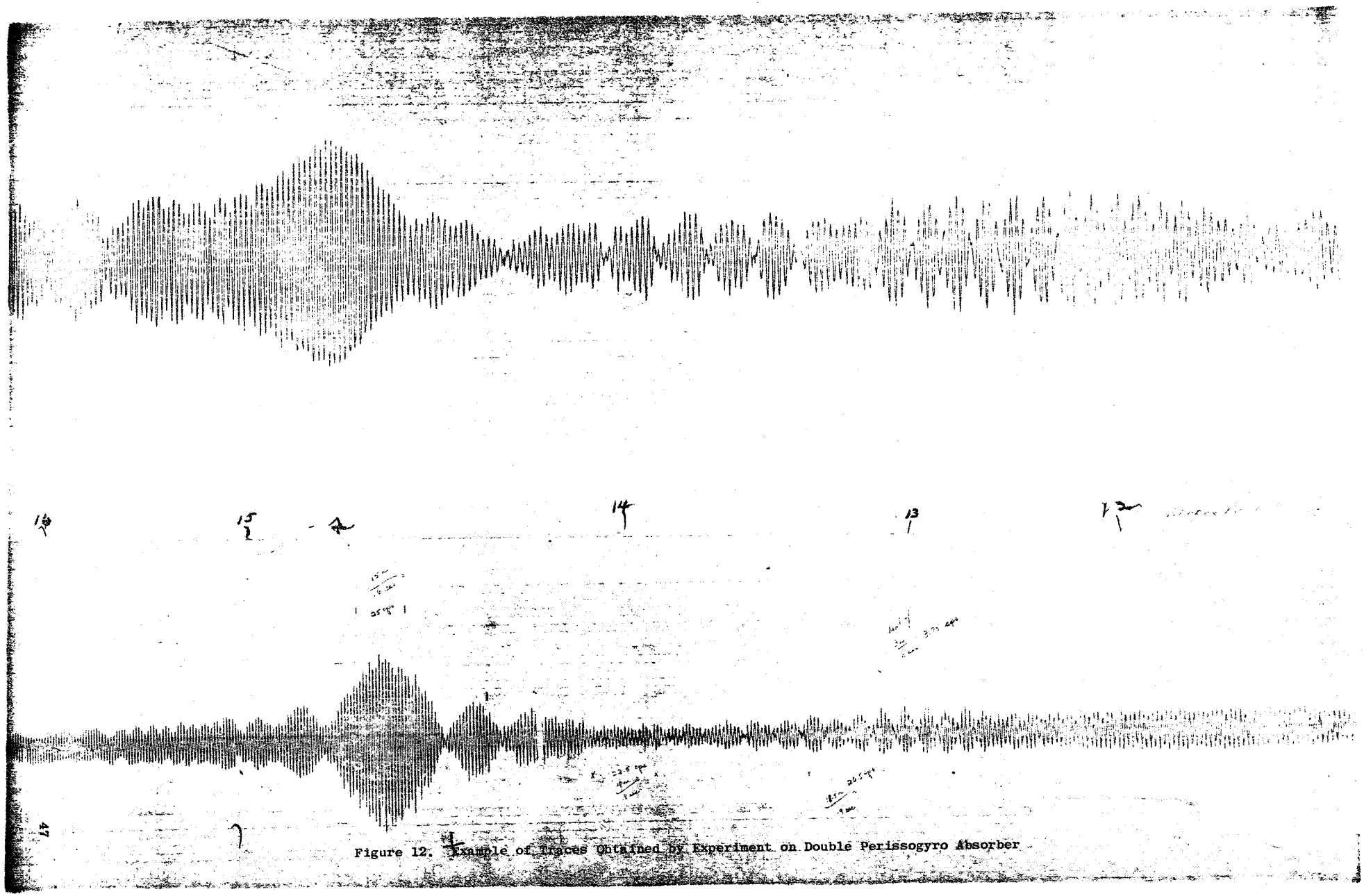

Figure 12. Example of Traces Obtained by Experiment on Double Perissogyro Absorber

TABLE 1

Experimental Model of the Single Perissogyro Absorber

Gyro Disc	Aluminum Plate 8" Dia.
Thickness of the disc	1/2"
Weight of gyro disc	2.44#
Length of steel rod	5-1/2"
Weight of motor assembly	24.2#
Weight of steel rod	.625#
Weight of universal joint	.24#
Weight of top plate	1.45#
Weight of connecting rod	1.50#
Weight of pick-ups	1.60#
Weight of shaker armature	2.00#

TABLE 2

Experimental Model for the Double Perissogyro Absorber

Gyro Disc	Steel Plate 8" Dia.
Thickness of the disc	1/2"
Weight of gyro disc	6.9#
Length of steel rod	3.75"
Weight of motor assembly	48.4#
Weight of two steel rods	.72#
Weight of two universals	.48#
Weight of top plate	2.90#

RESULTS AND DISCUSSION

Figures 13 and 14 show the principal features of the Perissogyro Vibration Absorber. Dimensionless values of amplitude are obtained by dividing the measured output by corresponding values obtained by shaking the Perissogyro absorber with the motor turned off. The latter data is termed X_p and indicates the response of the absorber as a pendulum. There is reasonable agreement between the theoretical and experimental results.

An examination of Figure 9 indicates that the theoretical null-rpm curves have two branches, one corresponding to a lower null and the other corresponding to a higher null. From the null equation for the single Perissogyro Vibration Absorber with $K=0=K_X$ i.e.

$$\omega^4\left(\frac{Mh}{I_X}-\frac{\bar{\bar{M}}}{Mh}\right)+\omega^2\left(-\Omega^2\frac{I_Z^2}{I_X^2}\frac{\bar{\bar{M}}}{Mh}+\frac{K_Y}{Mh}\right)-\frac{K_Y}{Mh}\Omega^2\frac{I_Z^2}{I_X^2}=0 \qquad (89)$$

It can be shown that there exist two null frequencies for each Ω, resulting in two distinct branches for the null-rpm curves. The lower branches approach asymptotically (i.e. as $\Omega\to\infty$), the value $K_Y/\bar{\bar{M}}$ whereas the upper branches approach asymptotically

$$\bar{\bar{M}}I_Z^2\Omega^2\Big/I_X(\bar{\bar{M}}I_X-M^2h^2) \qquad (90)$$

Also $\omega^2=0$, $\omega^2=K_Y/(\bar{\bar{M}}-M^2h^2/I_X)$ are the so-called static frequencies (i.e. when $\Omega=0$). The latter are the beginning values for the lower and upper branches respectively. An examination of Equation (89) indicates that as $K_Y\to\infty$, the null frequencies approach $\Omega I_Z/I_X$, which represents also the null frequencies for the "Double Perissogyro". This feature can be observed from Figure 9, where the null-rpm curves for the "Single Perissogyro" approach the corresponding curve for the "Double Perissogyro" as $K_Y\to\infty$. This is appropriate in view of the fact that a "Double Perissogyro" has always a null in the lateral direction; a condition which corresponds to having infinite lateral spring rate.

From Figures 13 and 14 it is evident that experimental results predict only the lower nulls. This feature was observed in all the experiments although a tendency to reach the higher nulls was noticeable. Such a tendency can be seen by examining the output trace presented in Figure 15.

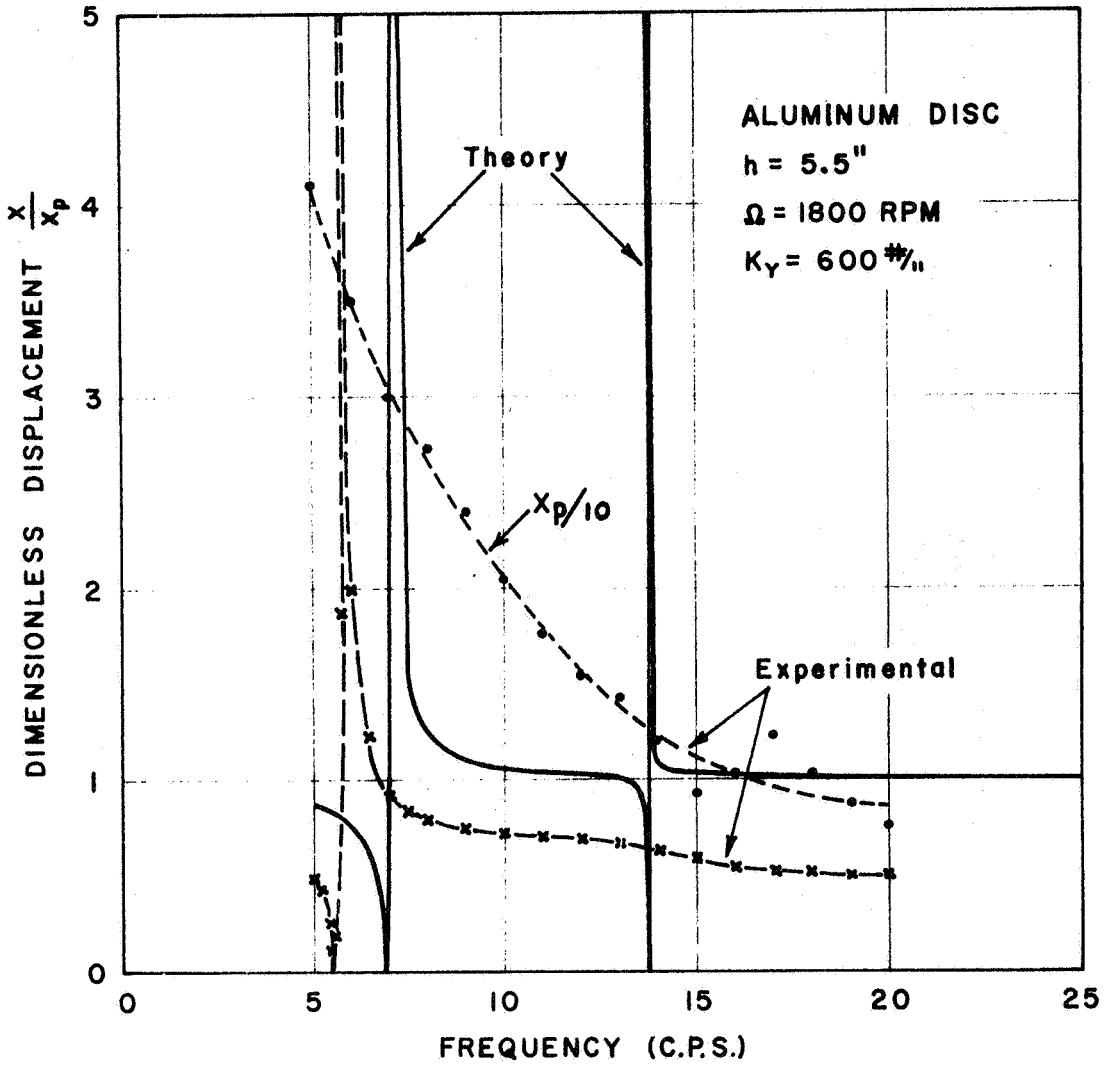

Figure 13. Theoretical and Experimental Response Curves (1800 rpm)

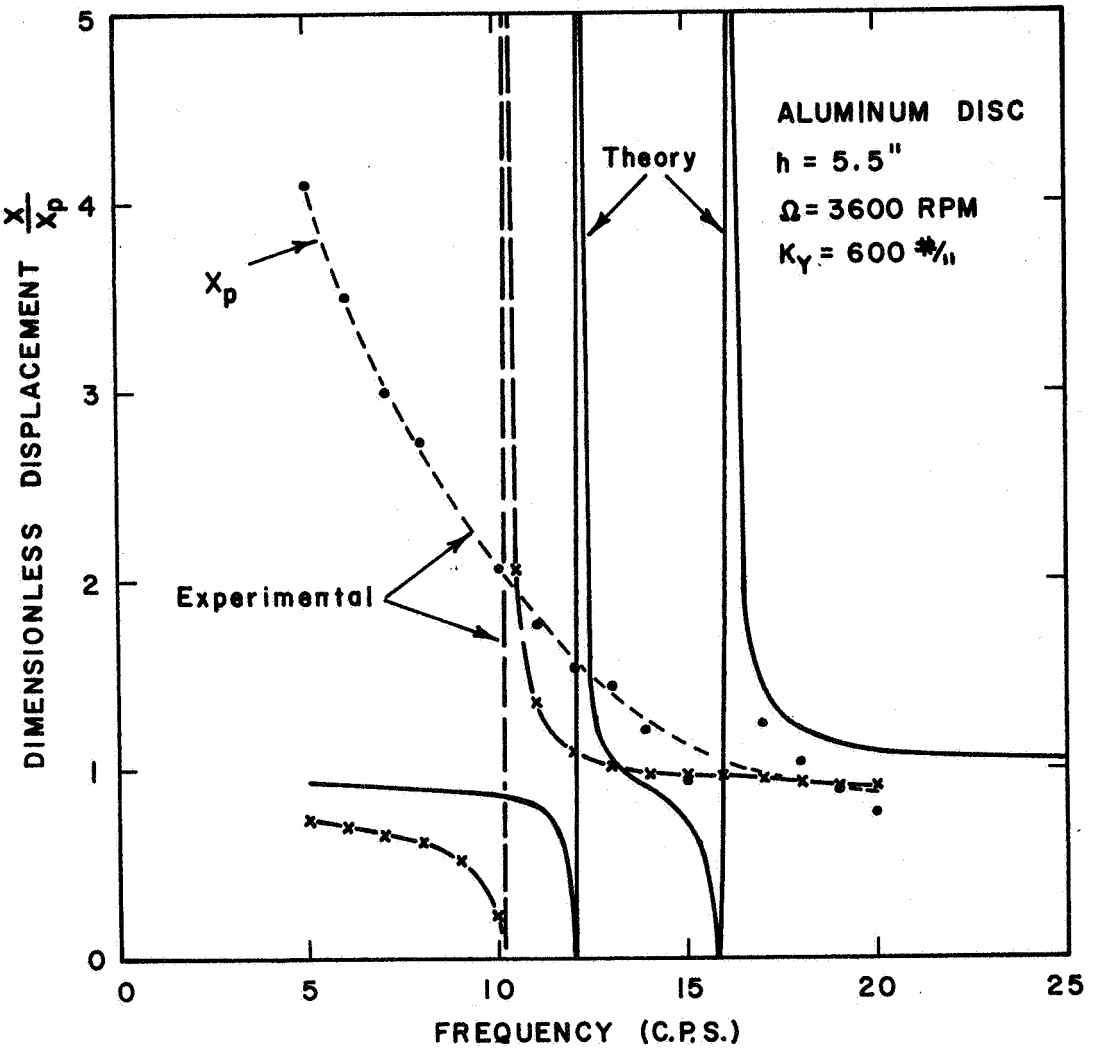

Figure 14. Theoretical and Experimental Response Curves (3600 rpm)

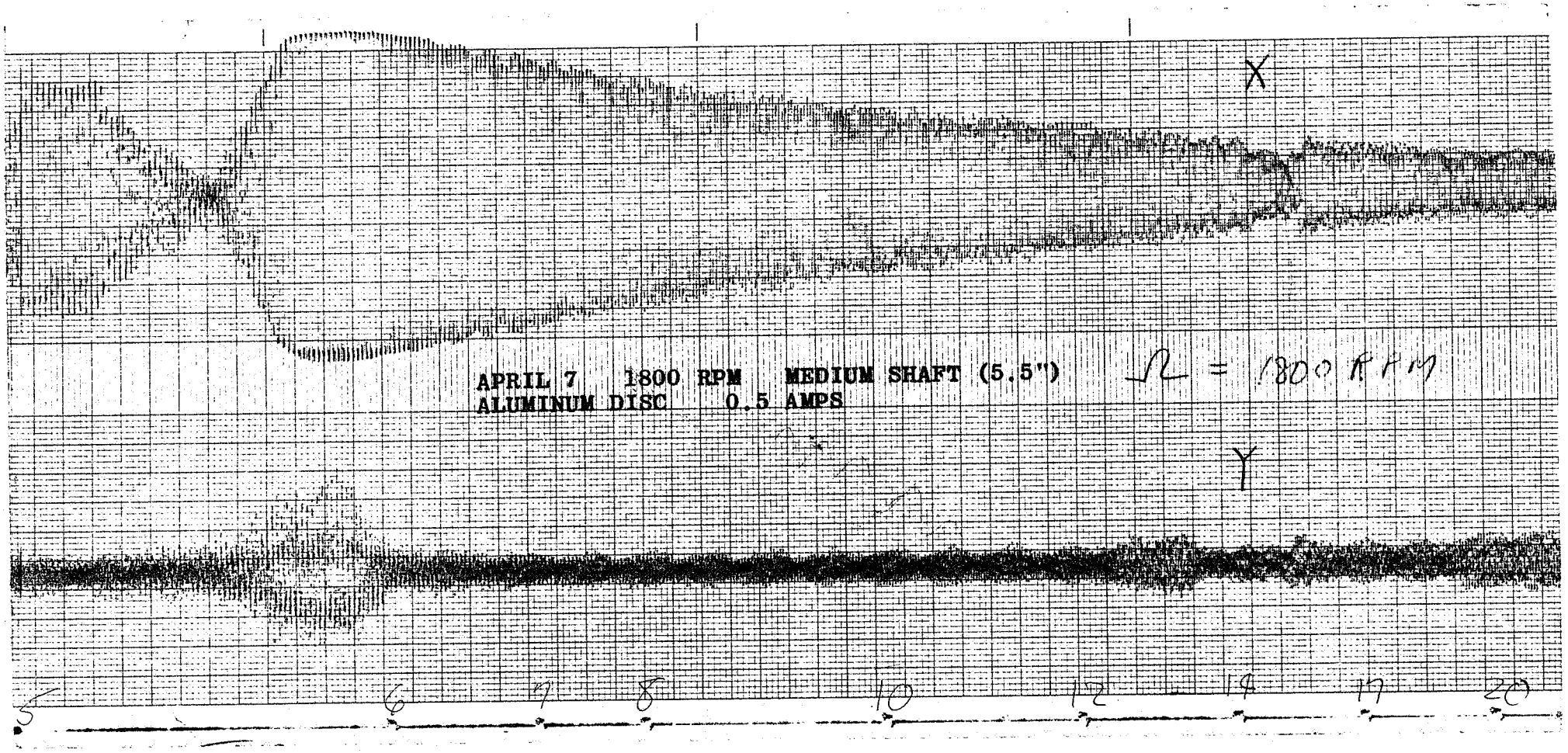

Figure 15. Example of a Trace Obtained by Experiment on Perissogyro Vibration Absorber

Figures 16 and 17 show the principal features of the Double Perissogyro vibration absorber. As before, dimensionless values (X/X_P) are plotted against the forcing frequencies and compared with corresponding values obtained by experiment. Unlike the Single Perissogyro, the Double Perissogyro provides a single null. Because of the problems referred to earlier in the report, repeated tests were necessary to obtain experimental results on the Double Perissogyro. Results of four such tests are plotted in Figures 16 and 17. The general trend shown by these experimental observations conform nearly to those suggested by theory. Actual nulls could not be determined accurately because of the influence of angular oscillations of the entire device (yaw motion) which resulted in a beating phenomenon. Limitations of time imposed on this project did not permit more thorough experimental work.

As observed earlier, one of the unique characteristics of a Gyroscopic Vibration Absorber is the synchronization possibilities it provides. For the Single Perissogyro, the null-rpm characteristics are linear only over a limited range of gyro speeds as may be seen from Figure 9. For the Double Perissogyro, however, the null-rpm relationship is linear for any range of gyro speeds. Thus a Double Perissogyro vibration absorber lends itself to linear synchronization, in addition to providing nulls in orthogonal directions. Details pertaining to such synchronization are presented at the end of this report and include the schematic of the necessary electronic circuitry.

Some of the questions that remain unanswered pertain to (1) self-excited oscillations that seem to start and persist in the gyroscopes under no input conditions for certain physical parameters of both the Single and Double Perissogyro Vibration Absorbers; (2) the beat phenomenon that seems to be induced at certain forcing frequencies on the Double Perissogyro vibration absorber. The answers to questions such as above and an understanding of the influences of various parameters such as mass ratios, spring rates, gyro speeds, inertias, etc. would have to be obtained by means of an extensive experimental program. Further theoretical research should include a rotation coordinate for the Double Perissogyro configuration in addition to including effects of damping.

Preliminary studies and calculations made on the "Coriolis Vibration Absorber" indicated null and natural frequencies so closely spaced that the device may be of questionable practical value. However, detailed parametric studies would be warranted before definite conclusions can be drawn.

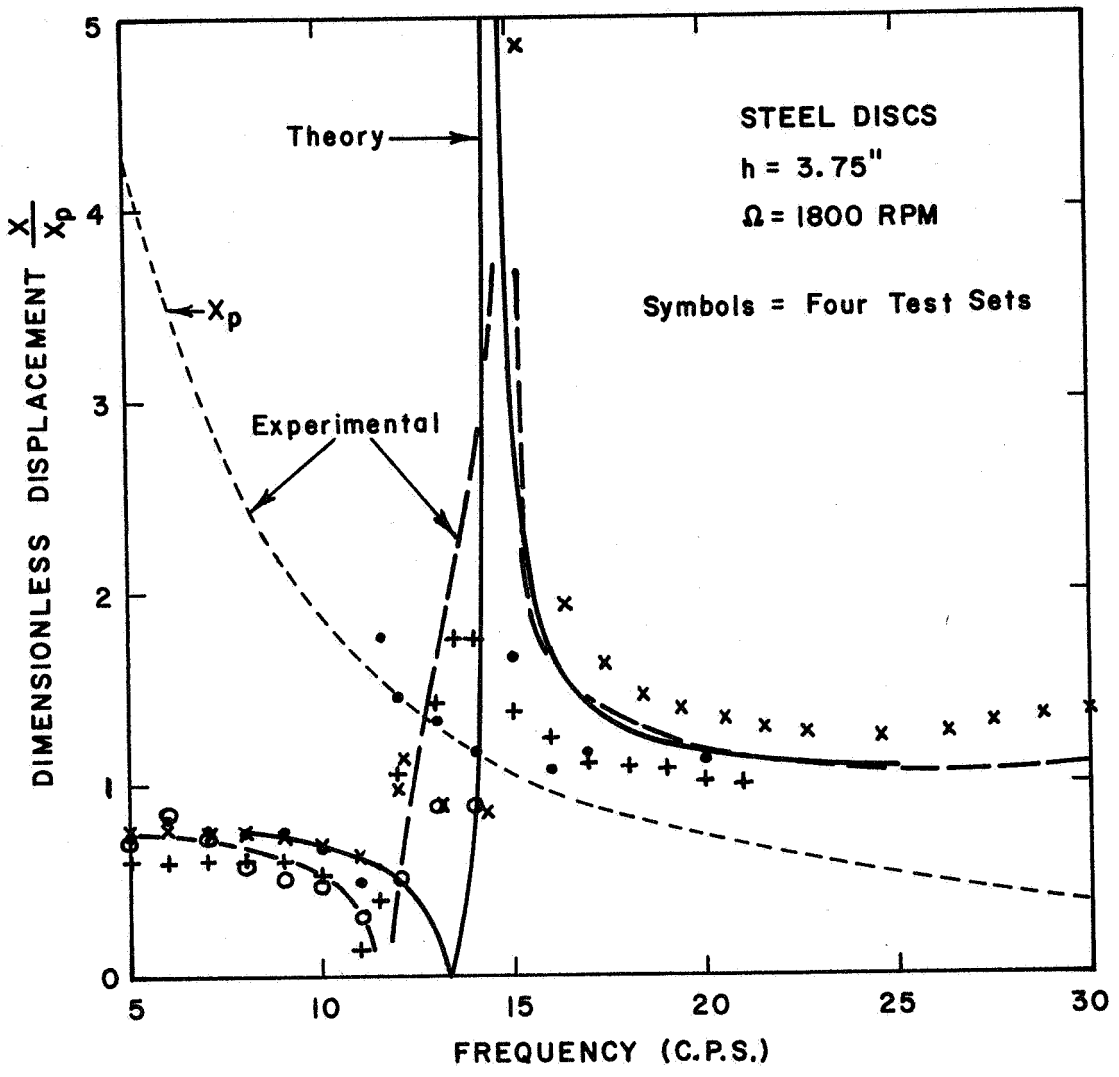

Figure 16. Theoretical and Experimental Response Curves for the Double Perissogyro Vibration Absorber

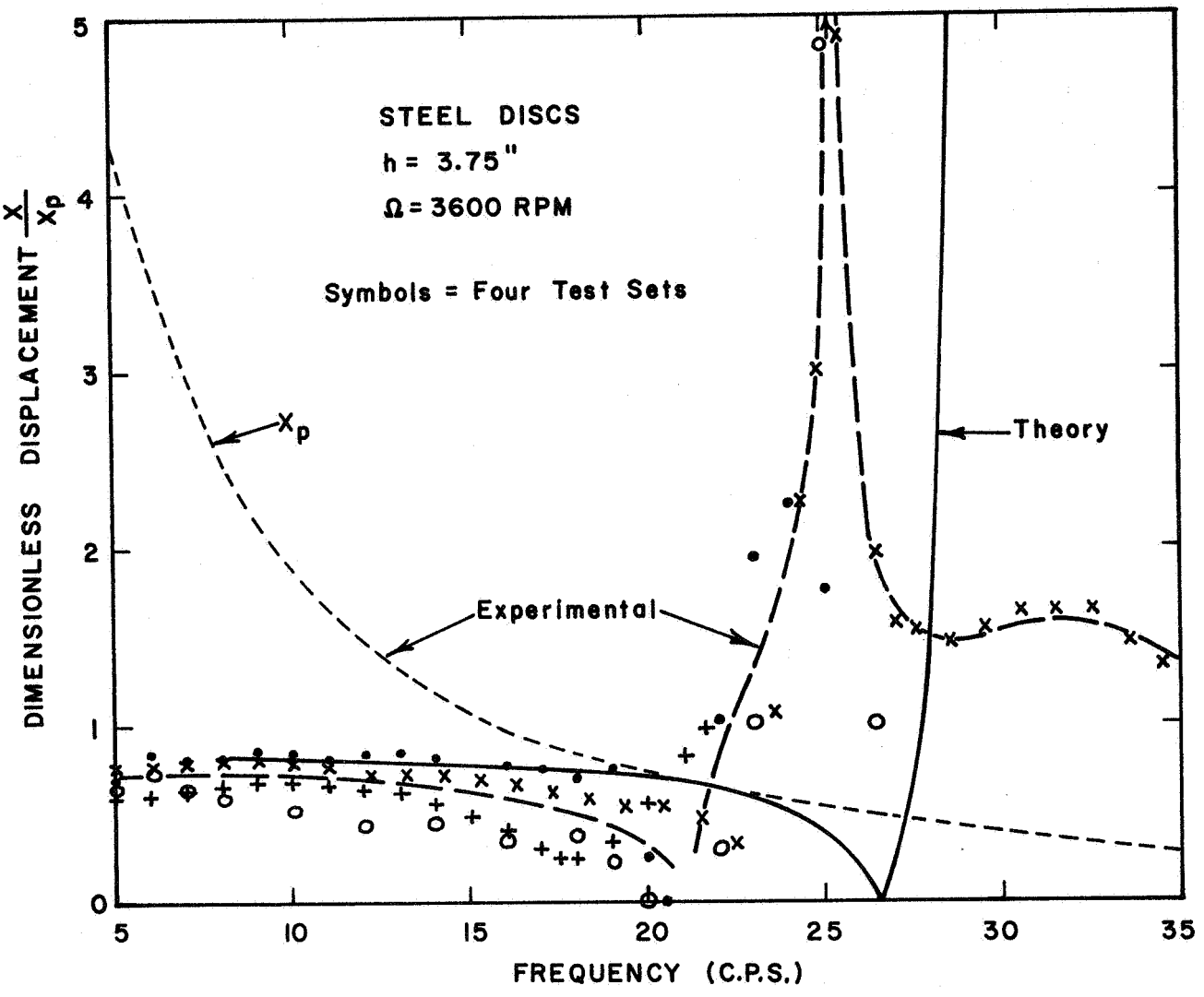

Figure 17. Theoretical and Experimental Response Curves for the Double Perissogyro Vibration Absorber

GYROSPEED SYNCHRONIZATION FOR "PERISSOGYRO VIBRATION ABSORBER"

In this section, details pertaining to synchronizing gyrospeeds are discussed. The general problem of synchronization may be stated as follows.

Given a relationship $\Omega = f(\omega_n)$ where Ω and ω_n represent gyrospeed and null frequency respectively, it is required to design an electronic circuitry which would automatically change the gyrospeed as soon as the excitation frequency changes.

In what follows the function $f(\omega_n)$ will be assumed as linear, i.e. $\Omega = C\,\omega_n$ where C is a constant which can be computed once the dimensions of the absorber are known.

A simplified block diagram of the proposed gyro speed synchronization system is shown in Figure 18. The reference shaft A and the controlled shaft B each have a gear/transducer combination to detect shaft speed. A magnetic pick-up (transducer) placed in close proximity to the teeth of a ferro-magnetic gear would be employed to generate an electrical signal whose frequency is proportional to the shaft speed. Since the transducers are rate sensitive, the output signal will vary in amplitude as well as frequency with shaft speed. Signal amplitude is also affected by gear tooth shape and tooth-to-transducer clearance. However, the speed control circuitry is only sensitive to the frequencies of the two incoming signals. Relative frequency detection is achieved by comparing the length of time required by each transducer signal to complete one cycle. This comparison is continuously repeated and averaged to produce a signal whose magnitude at any given time is proportional to the difference between the two frequencies. The system operates as a closed loop speed regulating servomechanism with short term proportional control plus integral compensation.

Amplifiers A1 and A2 in Figure 18 amplify and amplitude limit their respective transducer signals which are then coupled to the frequency detection circuits. The logic circuitry for each channel is identical and is composed of two clocked flip-flops which operate on the master/slave principle. The master/slave flip-flops allows information to enter the master while the trigger is high and transfers to the slave when the trigger goes low. Since operation depends only on voltage levels, any sort of wave shape may be used as trigger signals.

Assume flip-flops FF1 and FF2 initially in the clear mode with the set outputs low and the clear outputs high. The high clear output from FF2 is applied to the set input of FF1, however, assuming there is no trigger present FF1 cannot be set. The first amplitude limited pulse from A1 is simultaneously applied to the trigger inputs of FF1 and FF2. When this trigger is high, the master of FF1 is set but the output does not change state until the slave is set on the trailing edge of the trigger pulse. When the first trigger pulse is completed, the set input of FF1 is transferred to the set output and the clear output of FF1 becomes low. Since there was no set input to FF2, the trigger pulse had no effect on the output of FF2. After the first trigger pulse, there is a high set input to FF2 from the set output of FF1.

The second pulse from A1 cannot change the condition of FF1 since it has been previously set, however, FF2 can now be set since it has a high set input. Once both flip-flops have been set, further input pulses can have no affect on them until they are cleared. Since it took two consecutive input pulses to set both flip-flops, the time between the setting of FF1 and FF2 is equal to one input signal cycle or period. Gate 1 output is high only when FF1 is set and FF2 is clear, therefore, this pulse is equal in length to one input signal period. The logic circuitry for the B shaft signal performs in the same manner. The output pulses from Gates 1 and 2 are subtracted in summing amplifier A3 and averaged to produce a signal whose value is proportional to the difference in speed between shafts A and B.

When all four flip-flops have been set (one cycle each of A and B have been sampled), Gate 3 has a high on both inputs and enables the single shot flip-flop to clear all four flip-flops through their respective "direct-clear" inputs. The direct-clear input ($C\overline{D}$) overrides any normal synchronous set or clear signals, thus preventing simultaneous set and clear commands from producing unreliable outputs. Once all flip-flops have been reset (cleared), the sampling process is again repeated and the periods for signals A and B are compared on a one-to-one basis to produce an average error signal for the motor control circuit.

The synchronization circuitry is of the proportional plus integral type. Proportional control provides the short term stability required to cope with shaft speed transients, however, proportional only control requires a finite error to maintain servo motor drive. Integral control compensates for this error by adjusting its output to maintain shaft speed with zero error under steady state conditions.

It is possible to have shaft B operate at any multiple of shaft A's speed. This can be achieved in two ways.

The first method is to have the number of gear teeth on each shaft different so that the pick-up frequency will be identical at the desired speed ratios, e.g. if there were twice as many teeth on Gear B, shaft B would only have to rotate half as fast as shaft A to produce zero error signal (same output frequency). The second method is to bias the error signal at amplifier A3 to produce zero output at the desired speed or frequency differential; this could be accomplished with the "Speed Multiplier ADJ" shown in Figure 18.

The coarse speed adjustment shown in Figure 18 allows the speed of shaft B to be preset to its approximate operating value. The error detection circuits operate as a fine tuning and trim the speed of shaft B to the desired multiple of shaft A.

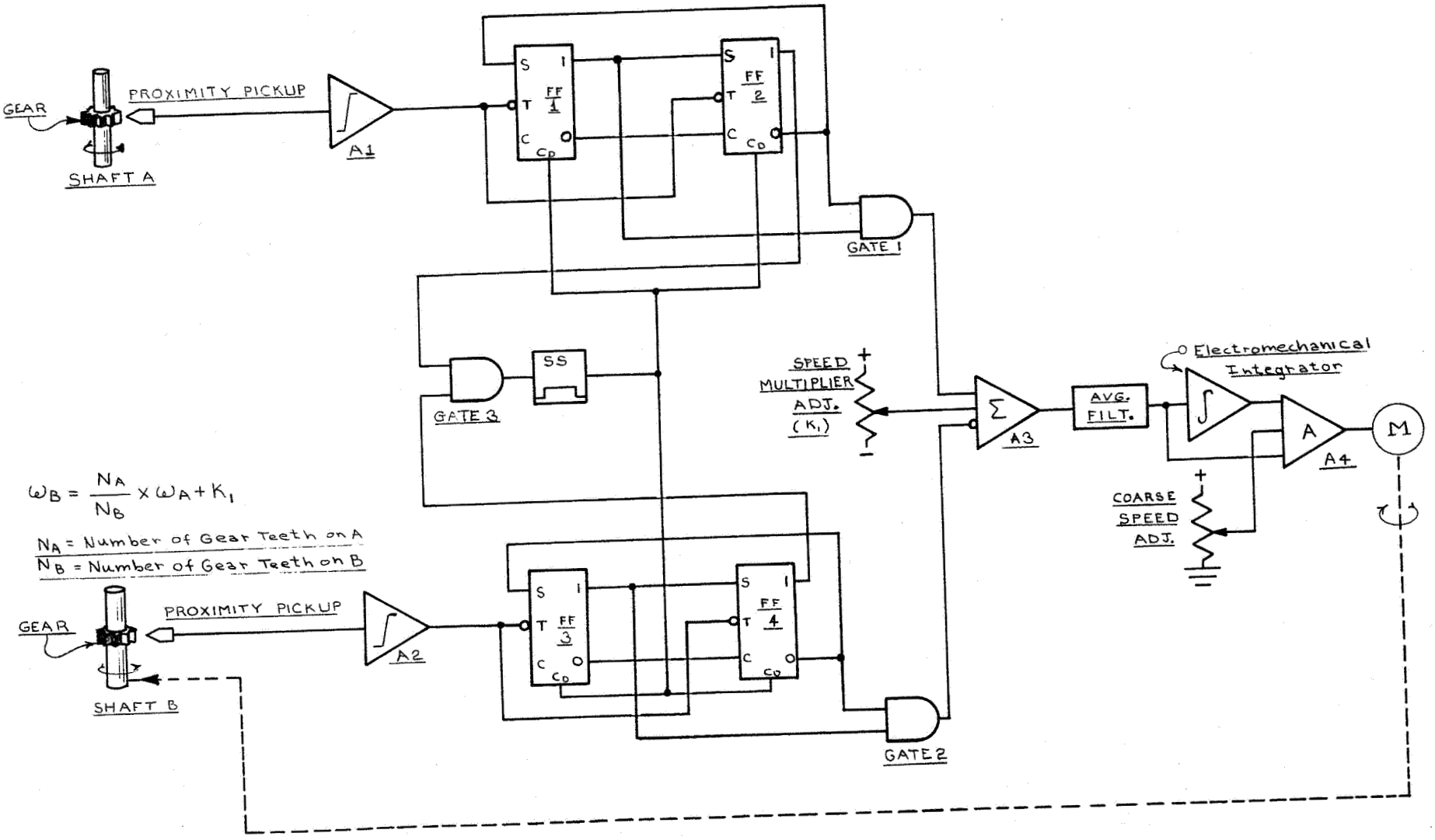

CIRCUITRY FOR LINEAR SYNCHRONIZATION OF GYROSPEED

Figure 18

PART 2

LIST OF SYMBOLS

C	Damping constant
C_C	Critical damping constant
C_r	Ratio C/C_C
f	Natural frequency of damped absorber/natural frequency of main mass
f_f	Favorable tuning frequency/natural frequency of main mass
f_o	Amplitude of the forcing function
g	Forcing frequency/natural frequency of main mass
h	Natural frequency of undamped absorber/ natural frequency of main mass
i	$\sqrt{-1}$
k_1	Spring constant of main spring
k_2	Spring constant of undamped absorber
k_3	Spring constant of damped absorber
m_1	Magnitude of main mass
m_2	Magnitude of undamped absorber mass
m_3	Magnitude of damped absorber mass
PQ P_1Q_1	Points on the response curves at which the amplitudes of main mass are independent of C_r
t	Time
x_1	Dynamic displacement of main mass
x_2	Dynamic displacement of undamped absorber mass

LIST OF SYMBOLS (Continued)

x_3	Dynamic displacement of damped absorber mass
x_{1st}	Static displacement of main mass
μ_2	Undamped absorber mass/main mass
μ_3	Damped absorber mass/main mass
ω	Forcing frequency
ω_1	Natural frequency of main mass
ω_2	Natural frequency of undamped absorber mass
ω_3	Natural frequency of damped absorber mass
φ	Phase angle

LIST OF FIGURES

Figure		Page
1	Parallel Vibration Absorber	68
2	Forces Acting on Each Mass	68
3	Amplitudes of Main Mass for Two Values of Damping When the Absorbers and the Main Mass are Tuned to the Same Frequency	79
4	Amplitudes of Main Mass for Two Values of Damping When the Absorbers are Favorably Tuned	80
5	Responses of the Absorber Masses When They are Tuned to the Same Frequency as the Main Mass	81
6	Responses of the Absorber Masses When They are Favorably Tuned	82
7	Responses of the Corresponding Conventional Absorber	83
8	Optimum Damping Ratio as a Function of the Mass Ratio μ	84
9	Phase Angle of the Main Mass as a Function of the Frequency Ratio ω/ω_1	85

SUMMARY

The analysis of parallel damped dynamic vibration absorbers is presented. The system considered is essentially a modification of the conventional damped vibration absorber and consists of adding, in parallel, a subsidiary undamped absorber mass in addition to the damped absorber mass. The analysis clearly shows that it is possible to obtain an undamped antiresonance in a dynamic absorber system which exhibits a well-damped resonance. While the bandwidth of frequencies between the damped peaks is not significantly increased, the amplitudes of the main mass are considerably smaller within the operational range of the absorber. The damped absorber mass and the main mass attain null simultaneously so that the vibratory force is transmitted to the undamped absorber.

Numerical results are presented for the special case when the absorber masses have the same magnitude. Two cases of tuning have been considered:

(1) when the absorber masses are tuned to the frequency of the main mass, and
(2) when the absorber masses are tuned to the so-called favorable tuning frequency.

Comparison of the results with those of the conventional absorber indicates that the parallel damped dynamic vibration absorber has definite advantages over the conventional damped vibration absorber.

INTRODUCTION

The conventional dynamic vibration absorber, first proposed by Frahm in 1909, is still quite widely used in practice because of its simplicity. The main drawback of the Frahm Absorber lies in the narrow bandwidth of excitation frequencies within which the absorber is effective. The purpose of many investigations that have followed since the introduction of Frahm absorbers has been either:

(1) to improve the effectiveness of the conventional absorber by suitable modification, or
(2) to invent entirely different and better devices in the hope of replacing the conventional absorber.

Gyroscopic vibration absorbers and impact dampers are but a few of the new devices that belong to the latter group. However, the only modification considered so far in the former group is the addition of damping to the absorber mass. The purpose of this report is to examine a further modification of the conventional absorber. Such a modification consists of adding, in parallel, a subsidiary undamped absorber mass in addition to the damped absorber mass. The system considered is shown in Figure 1.

The analysis that follows consists mainly of:

(1) the derivation of the governing equations of motion, and
(2) derivation of the condition for the amplitude of the main mass to be independent of the damping ratio .

The latter condition provides the frequencies at which the amplitudes of the main mass are independent of the damping ratio c/c_c . In addition, for the particular case of practical interest (i.e. when the absorber masses and the springs have the same value), the so-called favorable tuning (i.e. the tuning frequency at which the absolute value of the amplitudes independent of c/c_c is the same) has been determined in the form of a simple equation. Under this favorable tuning, the mass ratio required to provide the greatest spread between the frequencies is determined. Also, the equation which provides the optimum damping ratio (i.e. the ratio c/c_c at which the slope of the response curve is zero) has been derived.

Some of the equations in the analysis are rather lengthy and forbid hand computation. Therefore, the entire problem has been programmed on the computer. Numerical results obtained are presented graphically in dimensionless form.

ANALYSIS

The system under consideration with the forces acting on each mass is shown in Figures 1 and 2. The main mass is assumed to be subjected to the action of a periodic force $f_0 e^{i\omega t}$. Only steady state response is considered.

From Figure 2, the equations of motion can be readily written as:

$$m_1\ddot{x}_1 + k_1x_1 + k_2(x_1-x_2) + k_3(x_1-x_3) + C(\dot{x}_1-\dot{x}_3) = f_0 e^{i\omega t}$$

$$m_2\ddot{x}_2 + k_2(x_2-x_1) = 0$$

$$m_3\ddot{x}_3 + k_3(x_3-x_1) + C(\dot{x}_3-\dot{x}_1) = 0 \qquad (1)$$

For the steady-state response, the solutions X_1, X_2 and X_3 may be assumed as

$$X_1 = X_{1_0} e^{i\omega t}$$

$$X_2 = X_{2_0} e^{i\omega t}$$

$$X_3 = X_{3_0} e^{i\omega t} \qquad (2)$$

Substituting (2) in (1), a set of simultaneous equations in the unknowns X_1, X_2 and X_3 may be obtained. These equations may be represented in the form of a symmetric matrix as follows:

$$\begin{bmatrix} (k_1+k_2+k_3-m_1\omega^2+Ci\omega) & (-k_2) & -(k_3+Ci\omega) \\ (-k_3) & (k_2-m_2\omega^2) & (0) \\ -(k_3+Ci\omega) & (0) & (k_3-m_3\omega^2+Ci\omega) \end{bmatrix} \begin{bmatrix} X_1 \\ X_2 \\ X_3 \end{bmatrix} = \begin{bmatrix} f_0 \\ 0 \\ 0 \end{bmatrix} \qquad (3)$$

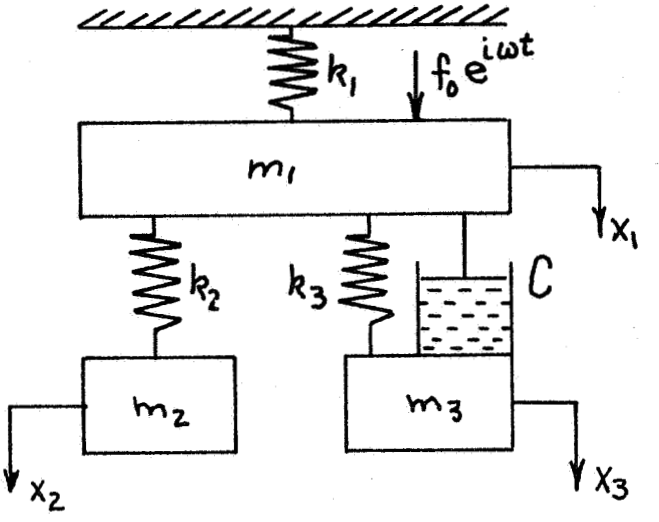

Figure 1. Parallel Vibration Absorber

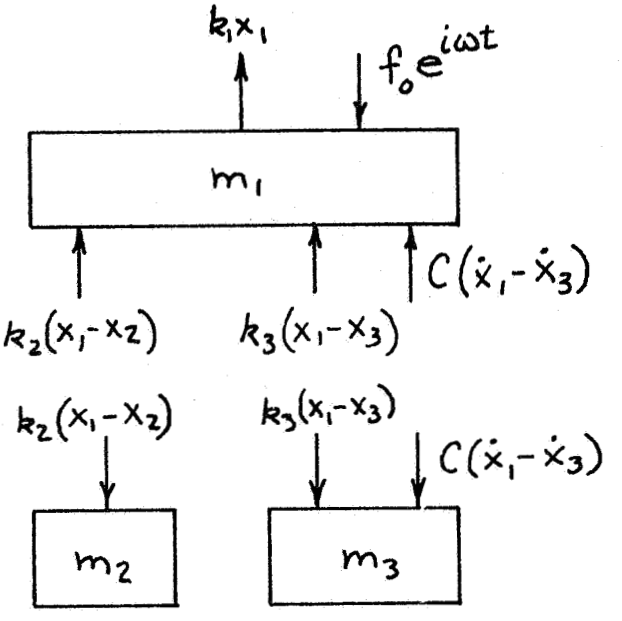

Figure 2. Forces Acting on Each Mass

Where k_1, k_2, k_3 are spring rates, m_1, m_2, m_3 are the masses and C is the damping constant. Solving for X_1 from (3) X_1/f_0 may be shown to be of the form:

$$\frac{x_1}{f_0} = \frac{A_1 + iB_1}{C_1 + iD_1} = \sqrt{\frac{A_1^2 + B_1^2}{C_1^2 + D_1^2}} \tag{4}$$

where

$$A_1 = k_2k_3 - k_2m_3\omega^2 + k_3m_2\omega^2 + m_2m_3\omega^4$$

$$B_1 = C\omega\,(k_2 - m_2\omega^2)$$

$$C_1 = (k_1 + k_2 + k_3 - m_1\omega^2)A_1 + k_2^2\,(m_3\omega^2 - k_3) + k_3^2\,(m_2\omega^2 - k_2)$$

$$D_1 = C\omega\left\{A_1 + (k_2 - m_2\omega^2)(k_1 + k_2 - k_3) - m_1\omega^2(k_2 + m_2\omega^2) - k_2^2\right\} \tag{5}$$

In order to represent the amplitude in dimensionless form, the numerator in Equation (4) may be divided by k_2k_3 and the denominator by $k_1k_2k_3$; the resulting expression for $X_1/X_{1_{ST}}$ may be written as follows:

$$\frac{x_1}{x_{1_{ST}}} = \frac{\left(1 - \frac{g^2}{f^2} - \frac{g^2}{h^2} + \frac{g^4}{f^2h^2}\right) + i2C_r\frac{g}{f^2}\left(1 - \frac{g^2}{h^2}\right)}{\left[\left\{\left(1 + \mu_2h^2 + \mu_3f^2 - g^2\right)\left(1 - \frac{g^2}{f^2} - \frac{g^2}{h^2} + \frac{g^4}{f^2h^2}\right) + \mu_2h^2\left(\frac{g^2}{f^2} - 1\right) + \mu_3f^2\left(\frac{g^2}{h^2} - 1\right)\right\} + i2C_r g\mu_3\left\{\left(1 - \frac{g^2}{f^2} - \frac{g^2}{h^2} + \frac{g^4}{f^2h^2}\right) + \left(1 - \frac{g^2}{h^2}\right)\right.\right.}$$

$$\left.\left.\left(\frac{\mu_2}{\mu_3}\frac{h^2}{f^2} + \frac{1}{\mu_3}\frac{1}{f^2} - \frac{1}{\mu_3}\frac{g^2}{f^2} - 1\right) - \frac{\mu_2}{\mu_3}\frac{h^2}{f^2}\right\}\right] \tag{6}$$

where $g = \frac{\omega}{\omega_1}$, $f = \frac{\omega_3}{\omega_1}$, $h = \frac{\omega_2}{\omega_1}$, $\mu_2 = \frac{m_2}{m_1}$, $\mu_3 = \frac{m_3}{m_1}$, $C_r = \frac{C}{C_C}$

$X_{1_{ST}} = \frac{f_0}{k_1}$ (Static displacement of main mass under the force f_0).

Similarly $X_2/X_{1_{ST}}$ and $X_3/X_{1_{ST}}$ may be represented in dimensionless form. Representing the denominator in Equation (6) by D

$$D\frac{X_2}{X_{1_{ST}}} = \left(1 - \frac{g^2}{f^2}\right) + i2C_r\frac{g}{f^2} \tag{7}$$

and

$$D\frac{X_3}{X_{1ST}} = \left(1-\frac{g^2}{h^2}\right)\left\{1+i2C_r\frac{g}{f^2}\right\} \tag{8}$$

It can be easily shown that X_1/X_{1ST} is independent of the damping ratio provided $(A_1/C_1) = \pm(B_1/D_1)$. Thus, the equations

$$A_1 D_1 \pm B_1 C_1 = 0 \tag{9}$$

may be used to obtain the values of at which the amplitudes of the main mass are independent of the damping ratio C_r. Substituting the expressions for A_1, B_1, C_1 and D_1 from Equation (6) in Equation (9), the resulting equations may be shown to be:

$$\begin{aligned}&(h^2-g^2)(f^2-g^2)\{\mu_3(h^2-g^2)(f^2-g^2)+(h^2-g^2)(1-g^2+\mu_2h^2-\mu_3f^2)\\&-\mu_2h^4\mp(h^2-g^2)(1-g^2+\mu_2h^2+\mu_3f^2)\}\mp(h^2-g^2)\{\mu_2h^4\\&(g^2-f^2)+\mu_3f^4(g^2-h^2)\}=0\end{aligned} \tag{10}$$

Omitting the minor details of calculation, the above equation may be shown to reduce to (when the minus sign is chosen):

$$\mu_3 g^4 (h^2-g^2)^2 = 0 \tag{11}$$

This is a trivial, but true, equation. According to Equation (11), the vibratory displacement of the main mass, X_1, is independent of damping when $g=0$, i.e. when the forcing frequency is zero or when $h=g$, i.e. when the forcing frequency is the same as the natural frequency of the undamped absorber mass.

Thus, the required non-trivial equation is obtained by choosing the plus sign in Equation (10), and may be shown to be:

$$\begin{aligned}&g^6(2+\mu_3)-g^4\{\mu_3(h^2+2f^2)+2\mu_2h^2+2(f^2+h^2)+2\}\\&+2g^2\{f^2h^2(1+\mu_2+\mu_3)+(f^2+h^2)\}-2f^2h^2=0\end{aligned} \tag{12}$$

Equation (12) is a cubic in g^2 and for given values of μ_2, μ_3, f and h, it may be solved to obtain the values of g at which X_1/X_{1ST} is independent of C_r. Using these values of g, the amplitudes of the main mass may be computed from Equation (6).

Although further analysis may proceed with all the parameters in their most general form, it is found that considerable simplification in computation results if the absorber masses and the corresponding spring rates are assumed to be equal. Also, such an assumption leads to one case of practical interest. With $\mu_2 = \mu_3 = \mu$ and $k_2 = k_3$, Equation (12) reduces to

$$g^6(2+\mu) - g^4\{f^2(4+5\mu)+2\} + 2g^2\{2f^2 + f^4(2+\mu)\} - 2f^4 = 0 \qquad (13)$$

With a little algebraic manipulation, Equation (13) may be shown to be:

$$\{g^4(2+\mu) - 2g^2(2\mu f^2 + f^2 + 1) + 2f^2\}(g^2 - f^2) = 0 \qquad (14)$$

Since $g = f$ corresponds to the null, the dimensionless frequencies, g, at which the amplitudes X_1/X_{1ST} are independent of damping are given by

$$g^4 - \frac{2g^2(2\mu f^2 + f^2 + 1)}{2+\mu} + \frac{2f^2}{2+\mu} = 0 \qquad (15)$$

Equation (15) is a quadratic in g^2 and provides the two required values of g (say g_1 and g_2). Using the values of g_1 and g_2, the corresponding values of the ratio X_1/X_{1ST} may be computed from a simplified equation obtained from Equation (6), i.e.

$$\left(\frac{X_1}{X_{1ST}}\right)_{g_1,g_2} = \frac{f^2 - g^2}{g^4 - g^2(1 + f^2 + 2\mu f^2) + f^2} \qquad (16)$$

Equation (16) is obtained from the general expression (6) by making the assumptions $\mu_2 = \mu_3 = \mu$, $f = h$, and by letting $C_r = 0$. The latter assumption is valid because at g_1 and g_2, X_1/X_{1ST} is independent of C_r.

The amplitudes at g_1 and g_2, as computed from Equation (16) are, in general, not equal. In order to avoid the necessity to refer to two different amplitudes and make comparisons at every stage, the absolute value of these amplitudes may be forced to be equal at g_1 and g_2. Because it is not apparent whether the amplitudes at g_1 and g_2 are of the same sign, the general requirement may be written as:

$$\frac{f^2 - g_1^2}{(f^2 - g_1^2)(1 - g_1^2 + 2\mu f^2) - 2\mu f^4} = \pm \frac{f^2 - g_2^2}{(f^2 - g_2^2)(1 - g_2^2 + 2\mu f^2) - 2\mu f^4} \qquad (17)$$

The solution of Equation (17) provides the value of the tuning (f) such that the absolute amplitude of the main mass at g_1 is the same as that at g_2. g_1 and g_2 are the magnitudes of the dimensionless frequency (forcing frequency/natural frequency of the main mass) at which the amplitudes of the main mass are independent of damping in the system.

Omitting the details of calculation, the required equations may be shown to be

$$(f^2 - g_2^2)(f^2 - g_1^2) + 2\mu f^4 = 0 \tag{18}$$

with the + sign and

$$(f^2 - g_1^2)(f^2 - g_2^2)(4\mu f^2 - g_1^2 - g_2^2 + 2) - 2\mu f^4 (2f^2 - g_1^2 - g_2^2) = 0 \tag{19}$$

with the - sign.

Clearly, only one of these equations is valid. The valid equation may be found as follows.

The roots g_1 and g_2 of the quadratic Equation (15) satisfy the conditions

$$g_1^2 + g_2^2 = \frac{4\mu f^2 + 2f^2 + 2}{2 + \mu}$$

and

$$g_1^2 g_2^2 = \frac{2f^2}{2 + \mu} \tag{20}$$

Equation (18) may be written as:

$$(g_1^2 + g_2^2) f^2 - g_1^2 g_2^2 - (1 + 2\mu) f^4 = 0 \tag{21}$$

Substitution of (20) in (21) leads to

$$f^4 (2\mu^2 + \mu) = 0 \tag{22}$$

Equation (22) is satisfied only when the absorbers have an uncoupled natural frequency of zero ($f = 0$), which is a trivial condition. Thus, the amplitudes (at g_1 and g_2) are opposite in sign, and the tuning f required to make them equal is obtained from Equation (19) written in the form shown below:

$$(g_1^2 + g_2^2)\{(g_1^2 + g_2^2) f^2 - 2\mu f^4 - g_1^2 g_2^2 - 2f^2 - f^4\}$$
$$+ 2g_1^2 g_2^2 (1 + 2\mu f^2) + 2f^4 = 0 \tag{23}$$

As before, substituting the expressions for $g_1^2+g_2^2$ and $g_1^2 g_2^2$ from Equation (20) in Equation (23), the resulting equation may be shown to be:

$$f^2 = \frac{1-\mu}{(1+2\mu)^2} \tag{24}$$

The required tuning, the so-called favorable tuning, which gives equal amplitudes can be calculated from Equation (24).

Under the "favorable tuning" condition, the values of g_1 and g_2 may be computed from Equation (14). In Equation (14), $g=g(f,\mu)$; however, when f is prescribed as "favorable tuning", $g=g(\mu)$ only. It would be of interest to determine the mass ratio μ which provides the greatest difference between g_1 and g_2. This has been done as follows:

$$g^2 = \frac{(2\mu f^2+f^2+1)\pm\sqrt{\{1+f^2(1+2\mu)\}^2-2f^2(2+\mu)}}{2+\mu} \tag{25}$$

Substituting the form of $f=\frac{\sqrt{1-\mu}}{1+2\mu}$, g_1^2 and g_2^2 may be shown to be

$$g_1^2 = \frac{(2+\mu)+\sqrt{3\mu(2+\mu)}}{(2+\mu)(1+2\mu)}, \quad g_2^2=\frac{(2+\mu)-\sqrt{3\mu(2+\mu)}}{(2+\mu)(1+2\mu)} \tag{26}$$

$$\therefore \quad g_1^2-g_2^2 = \frac{2\sqrt{3\mu(2+\mu)}}{(2+\mu)(1+2\mu)} \tag{27}$$

$\frac{d}{d\mu}(g_1^2-g_2^2)$ may be shown to be equal to

$$1-2\mu-2\mu^2 \tag{28}$$

Setting Equation (28) to zero, the required value of μ may be shown to be .366, i.e. 36.6% of the main mass is required for the absorber mass in order to attain a maximum bandwidth (g_1-g_2). Examining the second derivative of $g_1^2-g_2^2$, it is clear that $\mu=.366$ provides the condition for $g_1^2-g_2^2$ to be a maximum. However, such a mass ratio is too high and prohibitive to be of any practical use.

A similar expression can be derived for the case when $f=1$. For this case:

$$g_1^2 - g_2^2 = \frac{\sqrt{2\mu(3+2\mu)}}{(2+\mu)} \tag{29}$$

However

$$\frac{d}{d\mu}\left(g_1^2 - g_2^2\right) = 5\mu + 6 \tag{30}$$

From Equation (30), it is clear that there is no positive value of μ for which the equation is satisfied. Also, the second derivative of $g_1^2 - g_2^2$ in this case is positive, indicating a minimum condition rather than a maximum condition. Therefore $g_1^2 - g_2^2$ in this case increases continuously as μ is increased and does not attain an absolute maximum within the meaningful range of μ $(0 < \mu \leq .5)$.

In discussing the problem of damped vibration absorbers, it is customary to determine "optimum amplitude" and the corresponding "optimum damping". The "optimum damping" is defined as the damping required to obtain a zero slope of the response curve at g_1 or g_2. The resulting amplitude at g_1 or g_2 is termed "optimum amplitude". Den Hartog[3], in his analysis of a damped absorber, comments that the calculations involved in computing the "optimum damping" are "long and tedious". For the system described in this report, the calculations are much longer and more tedious. The optimum C_r $(C/C_c)_{OPT}$, is determined from the expression

$$\left\{\frac{d}{dg}\left(\frac{X_1}{X_{1_{ST}}}\right)\right\}_{g_{1,2}} = 0 \tag{31}$$

The calculations shown below are for the case when $\mu_2 = \mu_3 = \mu$ and $f = h$. g_1 and g_2 are, as before, the values of g at which $X_1/X_{1_{ST}}$ is independent of C_r.

$$\left(\frac{X_1}{X_{1_{ST}}}\right)^2 = \frac{A_1^2 + B_1^2}{C_1^2 + D_1^2} \tag{32}$$

where

$$\begin{aligned}
A_1 &= \left(f^2 - g^2\right)^2 \\
B_1 &= 2C_r\, g\left(f^2 - g^2\right) \\
C_1 &= \left(f^2 - g^2\right)\left\{\left(1 - g^2\right)\left(f^2 - g^2\right) - 2\mu f^2 g^2\right\} \\
D_1 &= 2C_r\, g\left\{g^4(1+\mu) - f^2 g^2(1+2\mu) + \left(f^2 - g^2\right)\right\}
\end{aligned} \tag{33}$$

[3] Den Hartog, "Mechanical Vibrations", Third Edition, McGraw-Hill Book Company, 1947.

$$\frac{d}{dg}\left(\frac{X_1}{X_{1ST}}\right)^2 = (C_1^2+D_1^2)\left\{A_1\frac{dA_1}{dg}+B_1\frac{dB_1}{dg}\right\}-(A_1^2+B_1^2)\left\{C_1\frac{dC_1}{dg}+D_1\frac{dD_1}{dg}\right\}=0 \tag{34}$$

$$\therefore \left[(A_1A_1'+B_1B_1')-\left(\frac{X_1}{X_{1ST}}\right)^2(C_1C_1'+D_1D_1')\right]=0 \tag{35}$$

where the primes indicate derivatives with respect to g.

In the following, the terms appearing in (35) will be listed in order, in their final form, and all details of calculation will be omitted.

$$A_1A_1' = -4g(f^2-g^2)^3 \tag{36}$$

$$B_1B_1' = 4C_r^2 g(f^2-g^2)(f^2-3g^2) \tag{37}$$

$$C_1C_1' = 6g^{11}-5g^9(2+4f^2+4\mu f^2)+4g^7(4\mu f^2+8f^2+12\mu f^4+6f^4+1)-12g^5(3\mu f^4+3\mu f^6+2\mu^2 f^6+3f^4+f^6+f^2)+2g^3(6f^4+8f^6+12\mu f^6+f^8+4\mu f^8+4\mu^2 f^8)-2g(2f^6+f^8+2\mu f^8) \tag{38}$$

$$D_1D_1' = 4C_r^2\{5g^9(1+\mu)^2-8g^7(f^2+3\mu f^2+2\mu^2 f^2+1+\mu)+3g^5(f^4+4\mu f^4+4f^2+4\mu^2 f^4+6\mu f^2+1)-4g^3(f^4+2\mu f^4+f^2)+f^4g\} \tag{39}$$

Substituting these expressions in Equation (35), an equation for optimum damping ratio ($C_{r\,OPT}$) can be obtained in in the following form:

$$C_{r(OPT)} = \sqrt{\frac{g^2h_1-h_2}{h_3-g^2h_4}} \tag{40}$$

where h_1 , h_2 , h_3 , h_4 are known functions of f and g and $\gamma = \frac{X_1}{X_{1ST}}$ computed at either γ_1 or γ_2 . The value of $C_{r(opt)}$ obtained from Equation (42) at g_1 is, in general, different from that at g_2 . An average value of $C_{r(opt)}$ is therefore proposed as the required optimum damping ratio.

DISCUSSION AND CONCLUSIONS

The responses of the main mass and the absorber masses have been represented graphically as functions of the frequency ratio γ with damping ratio C_r as parameter. Also, the phase angles of the main mass shown are computed and represented graphically. The responses for $f=1$ and $f=f_f$ are shown separately.

In order to judge the effectiveness of the parallel vibration absorber, the responses of the conventional absorber are compared with those of the corresponding parallel vibration absorber. The corresponding parallel vibration absorber is defined as the parallel vibration absorber whose absorber masses are each equal to one-half of the absorber mass of the conventional absorber.

An examination of Figure 3 shows the principal features of the comparison. The introduction of an undamped absorber mass, in addition to the damped absorber mass, has made it possible to obtain an undamped antiresonance in a dynamic absorber system which exhibits a well-damped resonance. This is an expected result and is decidedly an advantage. However, the amplitudes increase rather sharply for small changes in the frequency ratio γ, thus retaining the disadvantages of the conventional damped absorbers. Therefore, both the absorbers permit only very small tolerances in the change of the frequency ratio γ. Nevertheless, the parallel absorber appears to be superior to the conventional damped absorber if a comparison is made between the response curves for a damping ratio such as $C_r = .32$. The conventional absorber has, for this ratio of C_r, prohibitively large amplitudes within the operational range of the vibration absorber. Also, the characteristic feature of the response curve of the conventional absorber changes significantly in that the two smaller peaks for a low damping ratio such as for $C_r = .1$ tend to merge to a single, but larger, peak when C_r is increased. On the other hand, in the case of the parallel absorber, the characteristic features (i.e. two damped peaks and a null) remain intact when the damping is changed and the amplitudes within the operational range of frequencies are considerably smaller for higher damping ratios. Even for low damping ratios, it may be observed that the amplitudes in the narrow range between the peaks, P_1 and Q_1, are smaller.

In view of the fact that the above advantages are obtainable by merely assigning one-half of the absorber mass of the conventional absorber as the undamped mass of the parallel absorber, the device is obviously preferable.

Examination of the responses of the absorber masses shows that the main mass and the damped mass attain antiresonance simultaneously, thus transmitting the vibratory force directly to the undamped absorber mass. These response curves may be used in the design of the springs for the absorber masses such that the stresses induced are not too excessive.

Figure 8 represents the variations of "optimum damping" ratio as a function of the mass ratio. Clearly, the $(C_r)_{opt}$ required does not vary significantly from the corresponding $(C_r)_{opt}$ for the conventional absorber.

The procedures used to determine the "optimum amplitude" and "optimum damping" conform to those presented in Reference 3. The most favorable response curve (of the main mass) is therefore assumed to be the one which has a zero slope at the higher of the two points, P or Q. Accordingly, the best possible "resonant amplitude" at optimum damping is the ordinate at that point. However, it appears that there can be several different ways in which optimization can be defined. For example, a tuning condition and a desired damping may be found such that the second peak (i.e. at Q) may be made as small as possible. Similarly, it may be desirable to have the first peak (i.e. at P) as small as possible without any restriction imposed on the second peak. Such requirements may be of practical importance although the tuning condition obtained is not considered "favorable" according to the definition given earlier. The conditions stated above are, nevertheless, achievable with some judicious distribution of μ_2 and μ_3 (instead of simply making each of them equal to one-half of the mass of the equivalent conventional absorber).

These and other aspects of the parallel vibration absorber are recommended for further research.

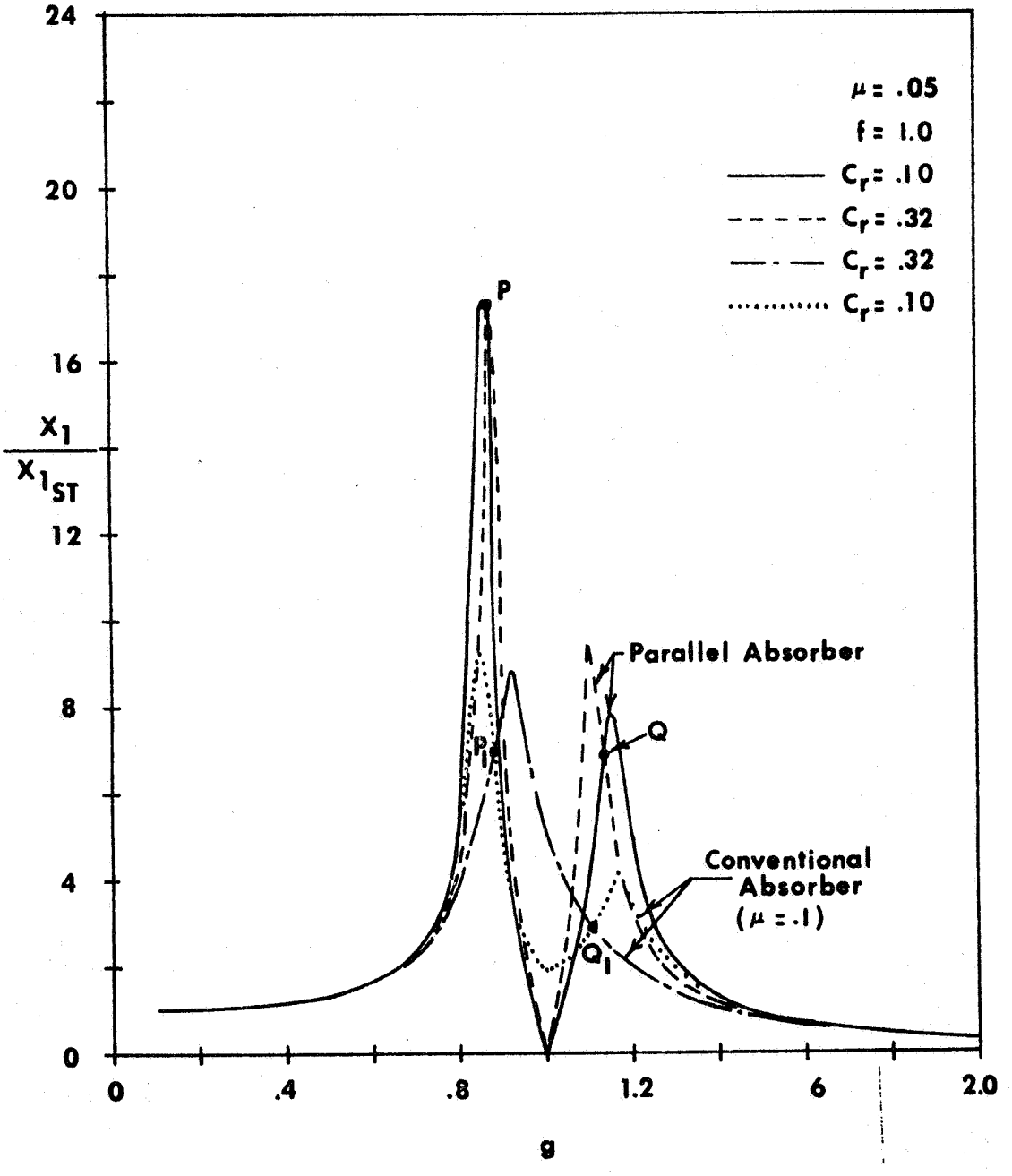

Fig. 3-Amplitudes of Main Mass for Two Values of Damping When the Absorbers and the Main Mass are Tuned to the Same Frequency.

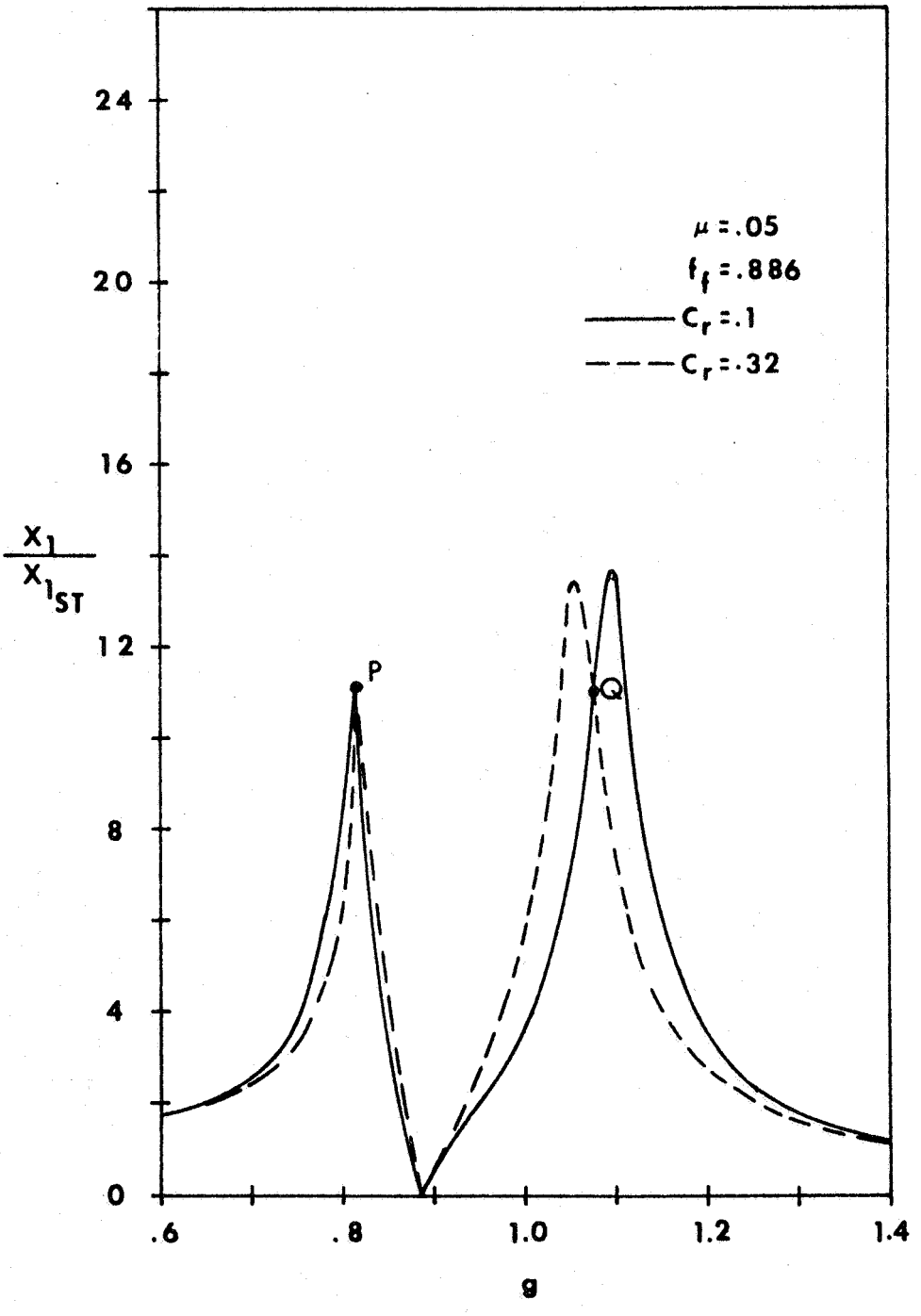

Fig. 4-Amplitudes of Main Mass for Two Values of Damping When the Absorbers are Favorably Tuned.

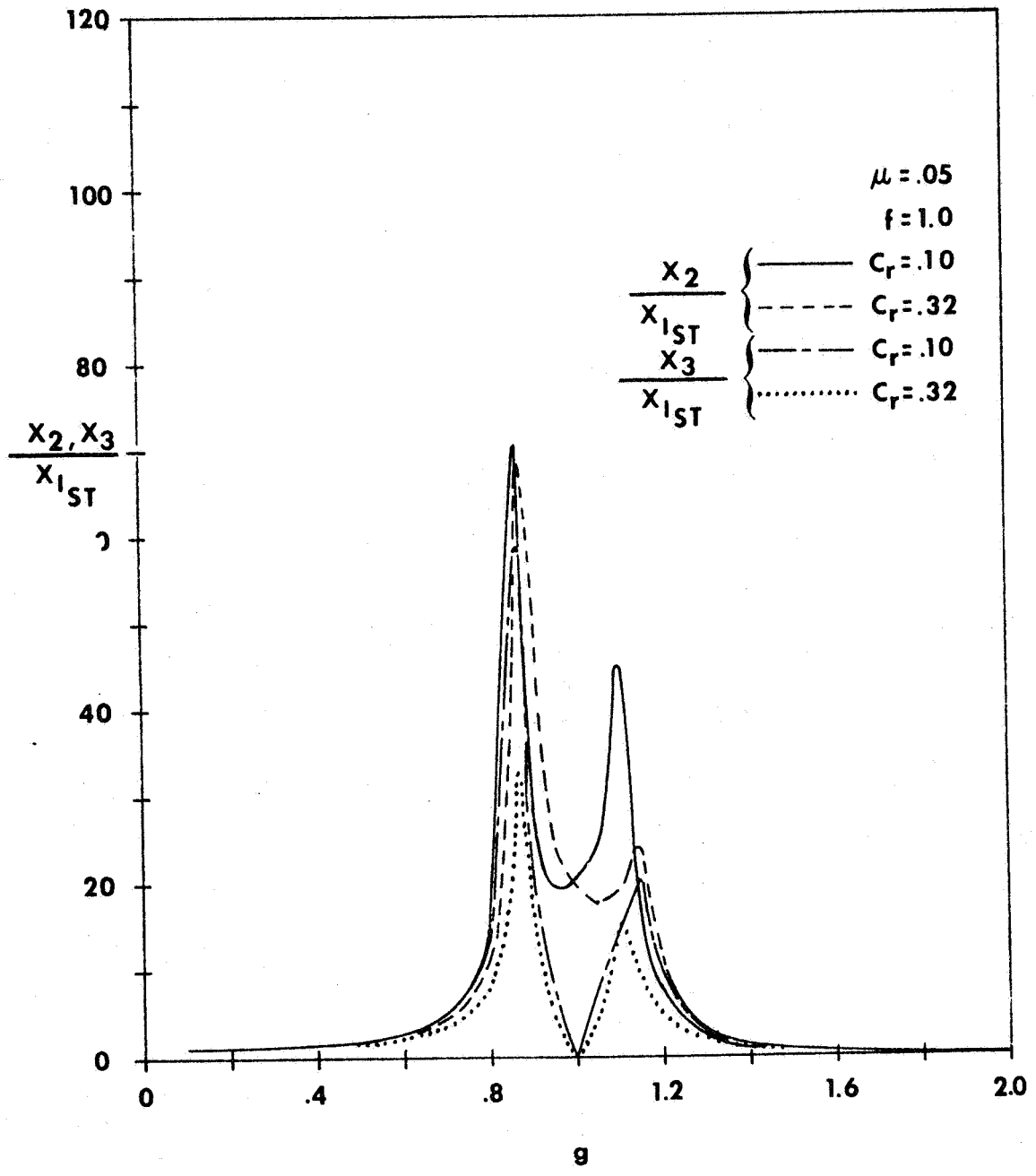

Fig. 5-Responses of the Absorber Masses When They are Tuned to the Same Frequency as the Main Mass

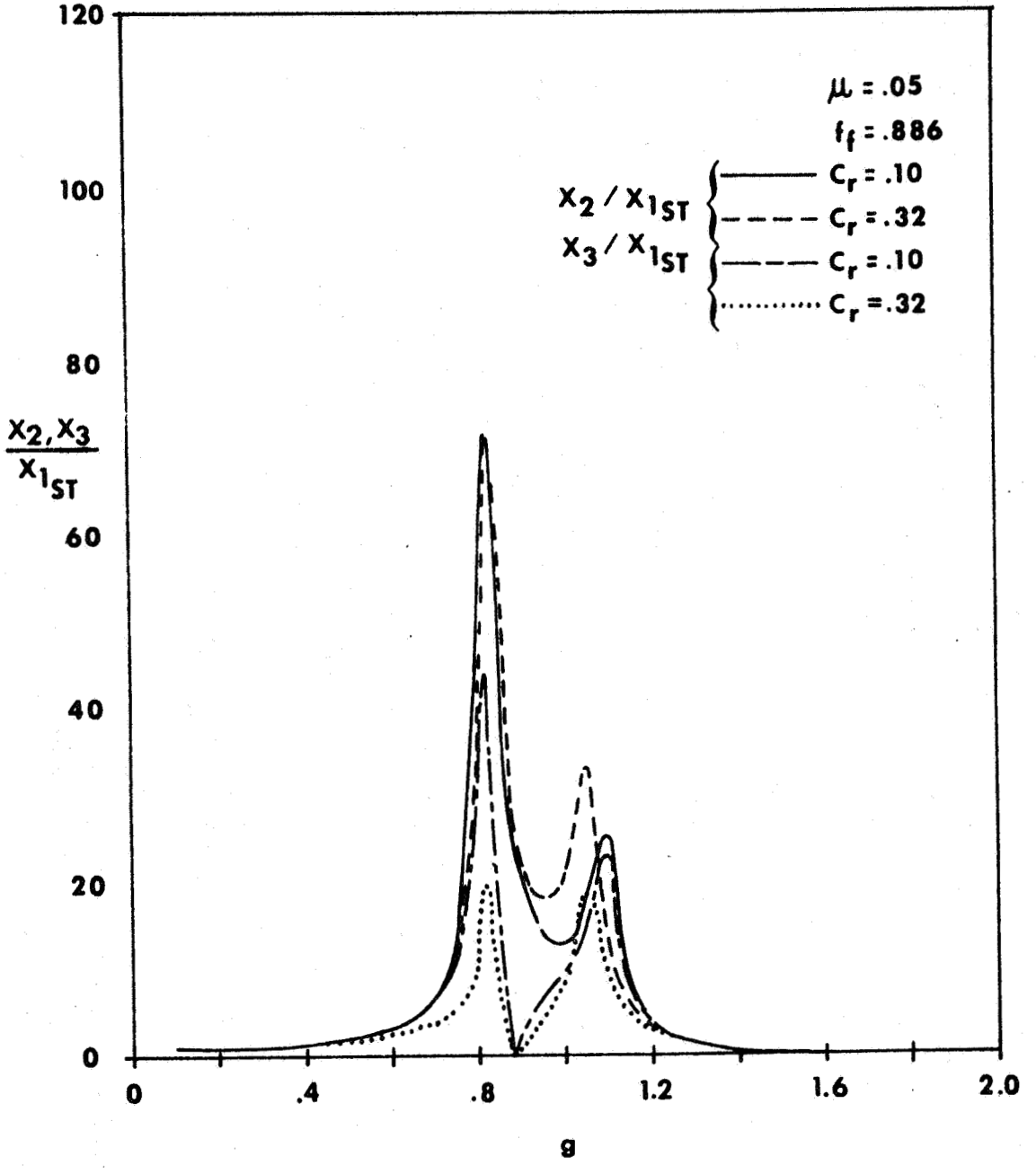

Fig. 6-Responses of the Absorber Masses When They are Favorably Tuned.

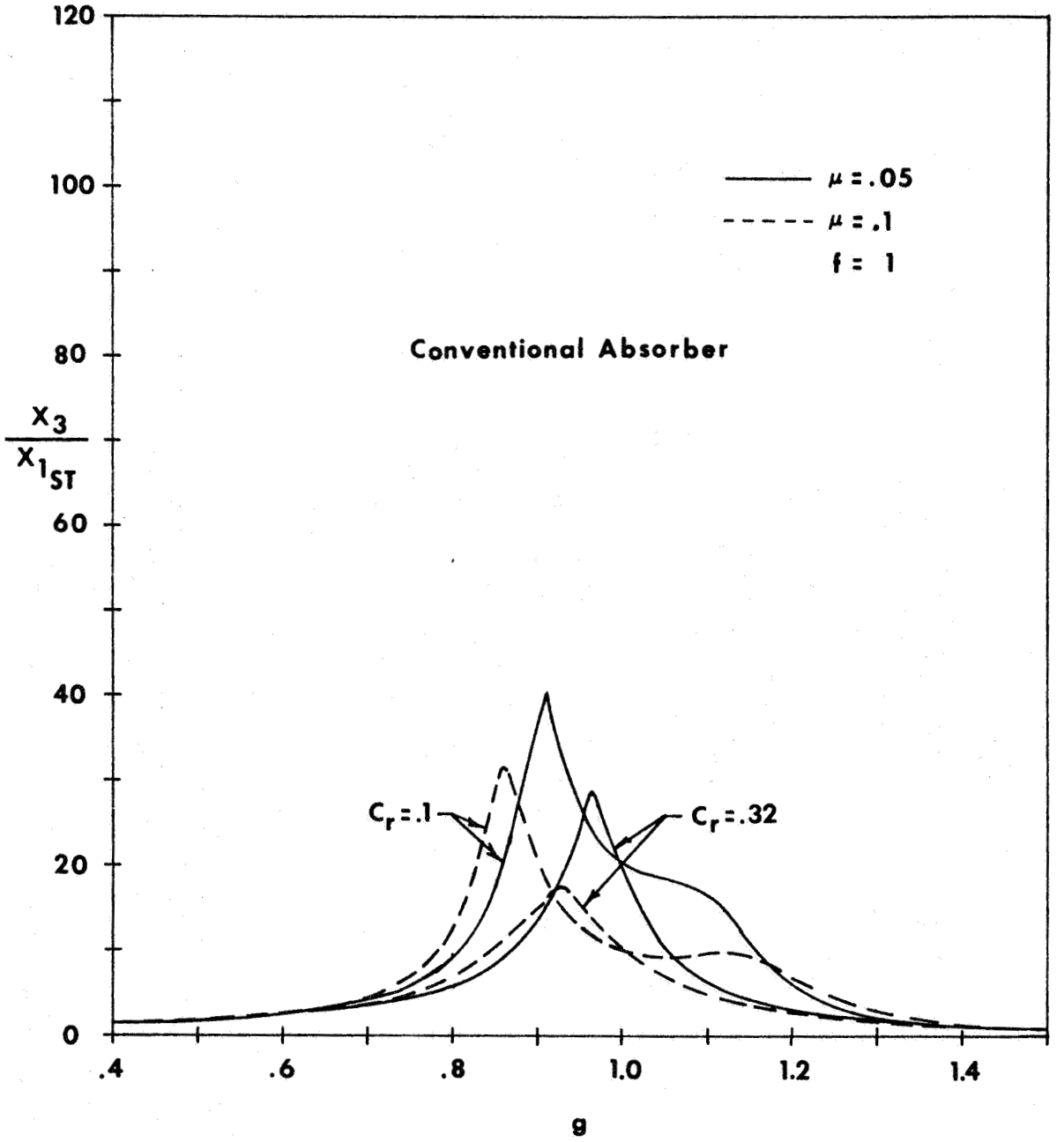

Figure 7. Response of the Corresponding Conventional Absorber

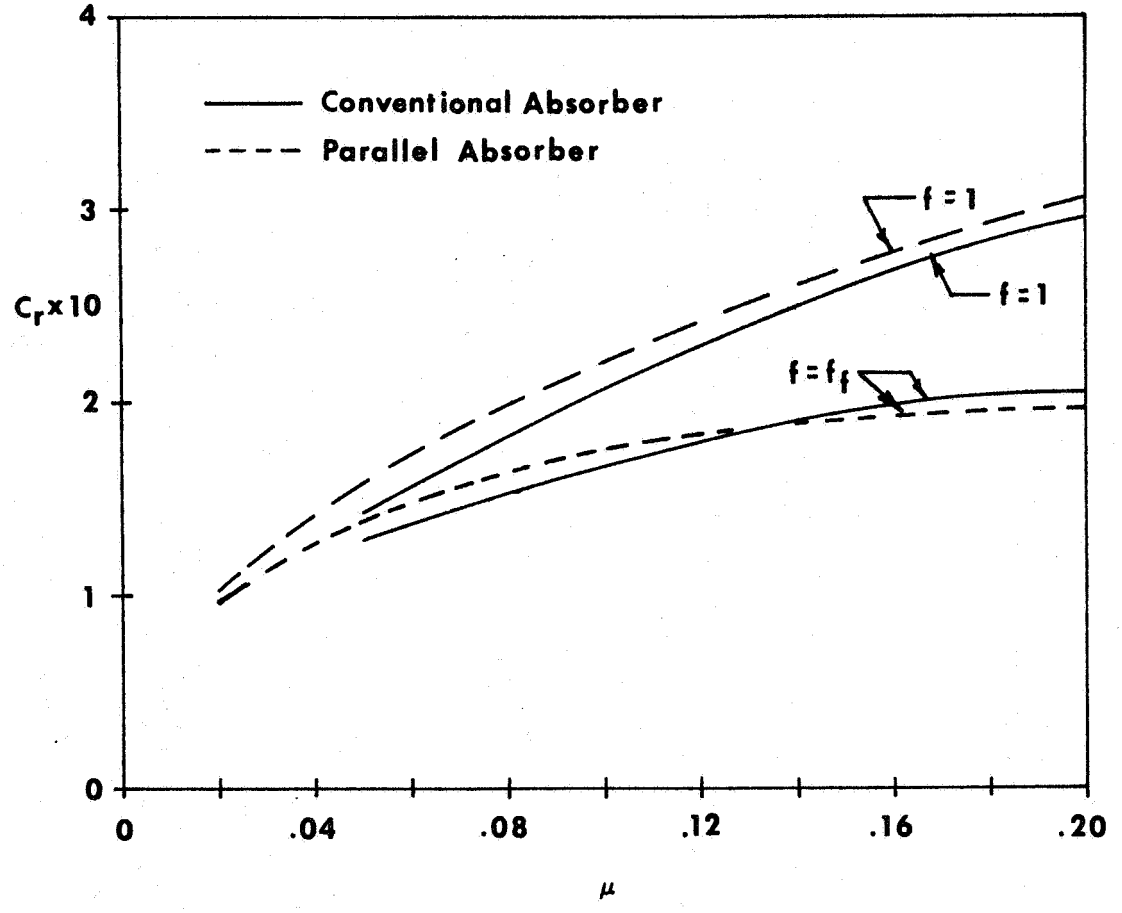

Figure 8. Optimum Damping Ratio as a Function of the Mass Ratio μ

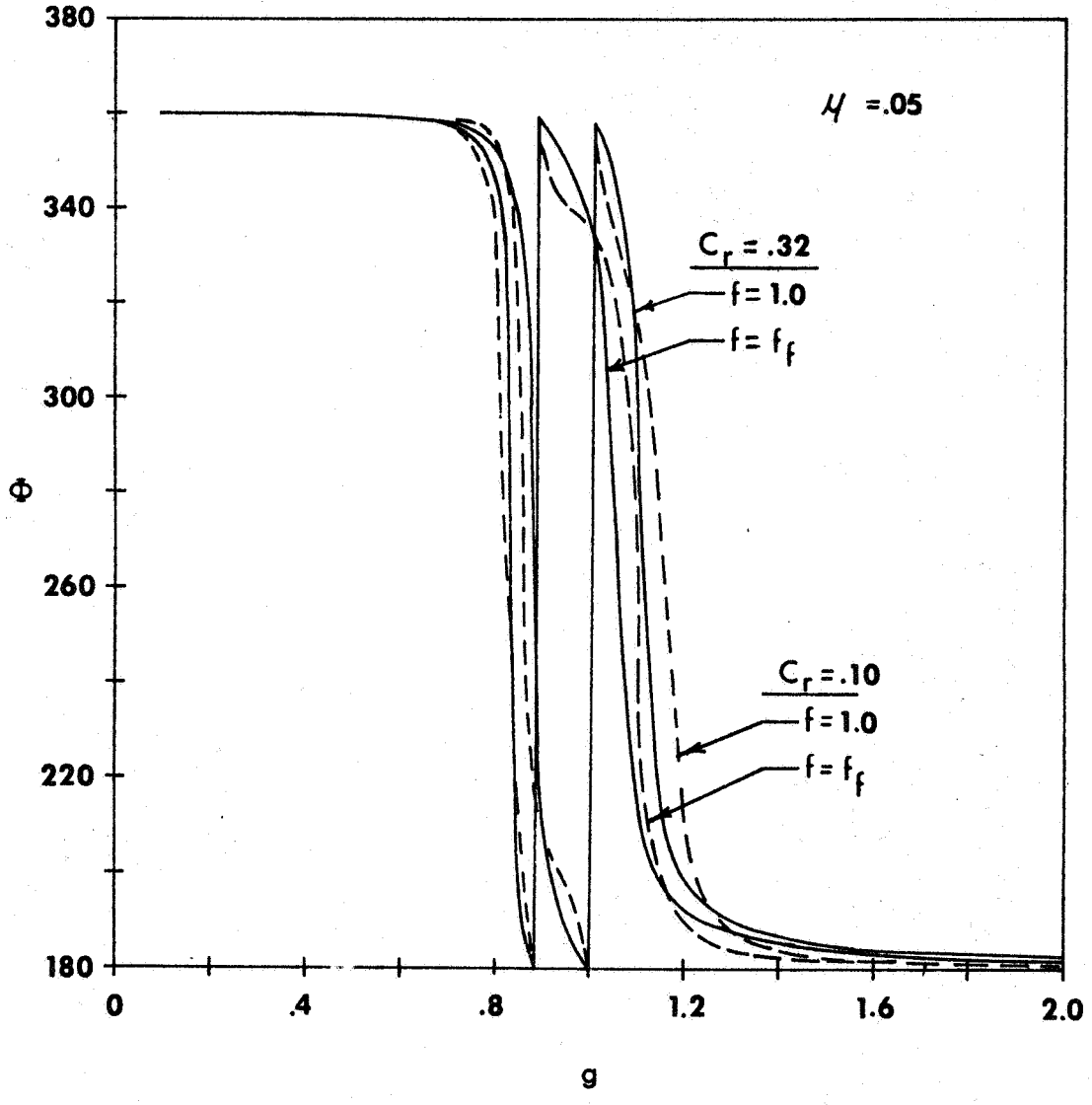

Figure 9. Phase Angle of the Main Mass as a Function of the Frequency Ratio ω/ω_1

ACKNOWLEDGEMENTS

The research work on which this report is based is performed by Kaman Aircraft, Division of Kaman Corporation, under Contract No. NASw-1394 for the National Aeronautics and Space Administration, under the direction of Mr. Harvey Brown. Grateful acknowledgements are due to Mr. Robert Jones and Mr. William Flannelly, Chief and Assistant Chief of Vibrations Research at Kaman, for their helpful criticism and discussion during the preparation of this report.

The details pertaining to synchronization studies were performed by Mr. Leonard Pauze of the Avionics Section of Kaman Aircraft.